University of Southern Queensland
Faculty of Engineering and Surveying

Vehicle Energy Usage

A dissertation submitted by

Mr Andrew Bellars
Student number : 0039732689

In fulfillment of the requirements of

Bachelor of Engineering - Mechanical

Abstract

The waste heat from exhaust gases and cooling systems of internal combustion engines can be an important heat source to provide additional power and improve engine overall efficiency. Developments and efficiency improvements in thermal electric generator technology has made recycling of this previously ignored energy source a viable proposition.

In this research project a design of an exhaust gas thermal electric generator is proposed. A computer simulation using CFD software ANSYS16.1 is conducted to estimate the expected performance of the system.

It is proposed that the Thermal electric generator output be used to charge the vehicle battery and thereby replace the conventional vehicle charging system. Additionally due to the continuous nature of the electrical power output it is proposed that electrical power also be utilized to power a hydrogen generation unit which will allow a controlled amount of hydrogen / oxygen mixture back into the engine under light throttle and lean burn conditions.

The design presented is estimated to produce a maximum power output of 2407 watts. This power output is comparable to that of a conventional vehicle charging system. The TEG design presented could be a suitable substitute for a conventional charging system. Additionally there are extensive fuel economy and emissions benefits in using the excess electrical power generated to power an electrolysis driven hydrogen generating cell.

University of Southern Queensland

Faculty of Health, Engineering and Sciences

ENG4111/ENG4112 Research Project

Limitations of Use

The Council of the University of Southern Queensland, its Faculty of Health, Engineering & Sciences, and the staff of the University of Southern Queensland, do not accept any responsibility for the truth, accuracy or completeness of material contained within or associated with this dissertation.

Persons using all or any part of this material do so at their own risk, and not at the risk of the Council of the University of Southern Queensland, its Faculty of Health, Engineering & Sciences or the staff of the University of Southern Queensland.

This dissertation reports an educational exercise and has no purpose or validity beyond this exercise. The sole purpose of the course pair entitled “Research Project” is to contribute to the overall education within the student’s chosen degree program. This document, the associated hardware, software, drawings, and other material set out in the associated appendices should not be used for any other purpose: if they are so used, it is entirely at the risk of the user.

Candidate certification

I certify that the ideas, designs and experimental work, results, analyses and conclusions set out in this dissertation are entirely of my own effort, except where otherwise indicated and acknowledged.

I further certify that the work is original and has not been previously submitted for assessment in any other course or institution, except where specifically stated.

Student name: Andrew Bellars
Student number: 0039732689

Signature

20/10/15

Date

Acknowledgements

I take this opportunity to express my gratitude to Dr Ray Malpress for all his help and support in enabling me to present this dissertation.

I would also like to thank my wife, Clair and sons, Darren, Jared and Dominic for their unceasing support during many years of studying.

Table of Contents

List of tables

List of figures

Chapter 1

Introduction

1.1 Introduction

With energy sustainability at the forefront of public and national concerns there is a pressing need to develop a better understanding of clean, safe alternative energy sources. Additionally our finite fossil fuel reserve need to be consumed as efficiently and sparingly as possible (Da Rosa, Aldo V, 2012). Internal combustion engines are a major consumer of our planets finite fossil fuel reserves. In California, approximately one-half of all the fuel reserves consumed, are for transportation – cars, planes, trucks, motorcycles, trains and buses. Of all the oil used in this state about three-quarters goes into making petrol and diesel fuel for vehicles (The Energy story, 2012).

As a result extensive research and development is devoted to finding alternative fuels for our engines and develop technology to improve the efficiency of current systems. There is much promise in electrical technology, however battery systems and electrical storage device development has limited the use of this technology so far. Electric motors are inherently more efficient than a heat engines. An electric motor could also be considered to be more environmentally friendly. This would depend on how the electric power is generated in the first instance. Solar power being somewhat emission free. Coal powered power stations, although they may have higher thermal efficiencies than an internal combustion (IC) engines, by the time power is relayed to the vehicle, this advantage is eroded (Da Rosa, Aldo V, 2012).

IC engines operating on easy to handle liquid fuel have been a very convenient power source over the last 120 years. This is likely to continue for many years to come. Emission levels have been a concern but could be largely offset by the use of renewable fuels such as Ethanol or Hydrogen, combined with well-developed and efficient emission control devices.

The main disadvantage of an IC engine is the relatively poor thermal efficiency. Of the total heat that is supplied to an engine in the form of fuel only 25% to 35% is converted into usable mechanical work. The remainder of this heat is wasted in discharged exhaust gasses or dissipated by the engine cooling systems (Yunus & Cengel, 2002). Effectively only 25 cents in every dollar spent on fuel is actually used to create power and 75 cents is completely wasted and discarded as wasted heat energy. Approximately 40% of this wasted thermal energy is discarded into the exhaust system. Statistics released by the ministry of public security in China showed that there were more than 240 million vehicles operating in China in 2012. This amounted to an annual fuel consumption of more than 270 million tons. The amount of wasted heat discharged into the exhaust system in 2012 in China alone amounted to a massive 107.6 million tons of fuel (Shengqiang B et al, 2014). Obviously a large percentage of the world's available fossil fuel reserves have already been depleted in this inefficient manner.

As fuel reserves become more limited, yet world economies continue to grow, it becomes more and more critical to use the fuel reserves that we have more efficiently. The purpose of this report is to evaluate thermal energy losses in an automotive context and to present a proposal for the recycling of exhaust gas waste thermal energy. An evaluation of the current thermal cycle processes used in an automotive application as well as power transmission heat loss is conducted. The amount of

thermal heat waste that is available for potential further use is quantified. Techniques for transforming thermal energy to electrical energy are discussed and analyzed with particular attention on the Seebeck effect thermal electric generators (TEG).

In this report a design of a thermal electric generator layout using the wasted thermal energy from an exhaust system is proposed. The design includes a solid model as well as an analytical and CFD analysis of the system. Possible designs to extract electrical power from the cooling system and vehicle torque convertor are discussed. It is proposed that the electrical power generated could be used to replace the vehicle charging system as well as power an electrolysis based Hydrogen production cell to improve vehicle fuel consumption.

1.1.1 Consequential effects of design

While it is anticipated that the thermal electric generator will increase overall thermal efficiency of an automotive internal combustion engine system, it is imperative that consideration be given to the consequential and ethical effects on society as a whole as well as the recyclability of the new component.

It is anticipated that the thermal electric generator will consist predominantly of aluminum alloy, which is readily available in all countries and easy to recycle. Thermal electric generator components are typical semiconductor materials and will need to be recycled in a similar manner to any other automotive electronic component.

The auto-electrical industry is a well-established industry with an extensive network of part suppliers, manufacturers and tradesman. If thermoelectric charging systems were to become a viable alternative to the conventional vehicle charging systems then many people may find their industry and employment opportunities dwindling. However the auto-electrical industry is also very dynamic and as many opportunities diminish, other arise. In recent times the focus of those involved in auto-electrical repairs has changed from being predominantly involved in starting and charging system repairs to more engine and body electronic related repairs and diagnosis. Starter motors and alternators have largely become cheaper to replace with a new part than to repair. The main component of the auto-electrical industry that could be effected would be the component manufacturers. As already mentioned there would be many opportunities in the manufacture of thermal electric generators and the drop off in demand for conventional charging system components would also diminish gradually. Additionally even though the thermal electric generator will have no moving parts and should be more durable than a conventional alternator, they will still operate in a harsh thermally fluctuating and corrosive environment. As with any other automotive component they will have a serviceable life. This may generate more employment opportunities for other related automotive industries such as exhaust fitters.

1.1.2 Risk assessment

Additional safety concerns will need to be considered in the design of an exhaust thermal generators and hydrogen generating cells. Hydrogen is highly flammable ($2H_2 + O_2 \rightarrow 2H_2O$). It can ignite in combination with as little as 23% air. Although petrol is also highly flammable it needs considerably more air to ignite and has a higher flashpoint. Hydrogen is also highly reactive and

combines readily with metals. Hydrogen piping and plumbing needs to be constructed of materials that are suitable. This material would normally be stainless steel which is relatively expensive.

Hydrogen generation cell output needs to be carefully monitored and controlled. Excessive production and/or storage could lead to explosion and fire hazard. Particular consideration needs to be given to the effects of an accident and/ collisions on the hydrogen cell.

While hydrogen has particular safety issues that need to be considered, it is still a fuel just like petrol, diesel and LPG and if all precautions are taken it can be considered as similar risk to any other fuel source. For the purposes of this project the quantity of hydrogen produced will be very small.

Effects of thermal generator on the efficient operation of the catalytic convertor need to be carefully considered and compliance with emission control regulations maintained. Visible emissions may be produced if the exhaust gasses are reduced to a temperature below the condensation point of the H_2O in the exhaust gasses. Careful consideration needs to be given as to how these can best be avoided or absorbed. This may not be an issue for individual vehicles moving at higher speed but numerous vehicles in slow traffic conditions may produce an excessive accumulation of visible steam vapor.

Heat and electrical wiring in close proximity may be a potential cause of electrical short circuit and fire hazard.

Risk associated with conducting this project can be considered as minimal as it is not anticipated that any component will be manufactured or tested.

1.1.3 Installation risk management plan

CE markings for hydrogen devices symbolize that the component conforms to the particular directive for the particular application. It is essential due to the nature of the device and public liability that a vehicle on board hydrogen generating device conforms to the prescribed requirements. Hydrogen systems shall comply with the following directives in order to gain CE marking status.

- Machinery directive; 98/37/EC
- Equipment and protection systems intended for use in potentially explosive atmosphere; 94/9/EC
- Pressure equipment directive; 97/23/EC
- Low voltage directive; 73/23/EEC
- Electromagnetic compatibility directive; 89/336/EEC
- Simple pressure vessel directives; 87/404/EEC and 90/448/EC

The most applicable to an automotive environment are the Machinery directive and the Equipment and protection systems directive.

1.1.3.1 Machinery directive summary 98/37/EC

- The manufacturer has to assess the risks of its system in normal and abnormal uses, and during running and maintenance operations.
- Materials and products shall not endanger exposed persons health and safety.
- Machinery shall be designed so as to facilitate its safe handling, packaging and storage.
- Control systems shall be safe and reliable.
- Safety shall be taken into account.
    - For the design, localization, signals of the control devices.
    - For the starting, restarting and modification of the running.
    - For the stopping procedures, normal and emergency.
- Prescription given to ensure safety of device in case of power failure.
- Moving parts and equipment shall be designed to avoid hazards. Where hazards persist adequate guards or protective devices shall be fitted.

1.1.3.2 Hydrogen generator design layout principles

- Hydrogen generator to be located where there is minimum risk of hydrogen/air accumulation.
- Appropriate insulation or shielding to minimize absorbing of heat to the device.
- Appropriate control of hydrogen generator to ensure hydrogen generation only can occur during required operational conditions.
- Appropriate instruments and warning devices to monitor generator correct operation.
- Appropriate monitoring and control of water supply to hydrogen generator.

Risk management chart based on anticipated hydrogen production of 0.5kg/hour	**People at risk**	**Risk level**
General hydrogen storage and production in vehicle during normal use	Vehicle occupants	low
Hydrogen during accident	Vehicle occupants / pedestrians	low
Heat and electric wiring	Vehicle occupants	low
Visible emissions	Other vehicle operators	low
Corrosion	Vehicle occupants	low

1.1.4 Timeline

Timeline for project completion.

- Project allocation due11 March 2015
- Project specifications due18 March 2015
- Preliminary report submission date 03 June 2015.
- Complete detailed solid model completed 30 August 2015
- Heat simulation analysis on aluminum core completed 30 August 2015
- Preparation for project presentation to peers 30 August 2015
- Partial draft dissertation 16 September 2015
- Dissertation submission 29 October 2015

Chapter 2

Vehicle system energy waste

2.1 Introduction

Most vehicle system inefficiencies present themselves as wasted heat energy. The most noticeable of these are the waste heat from the vehicle exhaust and cooling systems. This project will focus primarily on the recycling of the wasted thermal energy from the exhaust system, however similar techniques could be applied to other areas of thermal heat loss to recycle the thermal energy. Other areas of significant thermal energy loss in a vehicle include:

2.1.1 Cooling systems

In a perfect world the engine cooling system would not be necessary. We would simply make our engines out of materials that produce minimal friction and have infinitely low thermal conductivity. Heat from combustion would not be able flow into our engine materials which would be good insulators and be able to withstand extreme temperatures without any component failure. Unfortunately despite extensive research in the application of ceramic materials in engine components design, at this present time engine material remain primarily Steel and Aluminum alloys. Steel and Aluminum alloys both have relatively high thermal conductivity and are susceptible to failure at extreme temperature. The only advantage of these materials being that they are readily available and easily cast into complex shapes. As a result the heat generated and dissipated in the cooling system is a direct result of component and material inefficiencies. As much as 30% of the available heat energy in the fuel is dissipated and wasted in the cooling system. In money term this is 30 cents in every dollar spent on fuel completely wasted. At this present moment in time no vehicle manufacturer has a production vehicle that recycles this wasted heat energy. The only major use of the cooling system heat has been to drive the vehicle cabin heating system.

2.1.2 Torque convertor

The torque convertor is a fluid drive system used on an automatic transmission to transmit the torque from the engine to the transmission. During acceleration the impellor (input) drives the turbine (output) via the transmission fluid. During this stage there is a large amount of slip between the impellor and turbine which results in heat being generated. The amount of heat generated depends on the amount of slip, the design of the torque converter and torque converter to engine compatibility. Torque convertor inefficiencies occur initially at stall. Stall is the condition when the turbine is not rotating and engine speed is at the torque peak. Efficiency is improved as the turbine increase in speed and then drops off again as the impeller and turbine reach similar speeds. When the turbine approaches the impeller speed this is referred to as coupling point.

Table 1 Torque converter efficiency curve (JM clutches and converters)

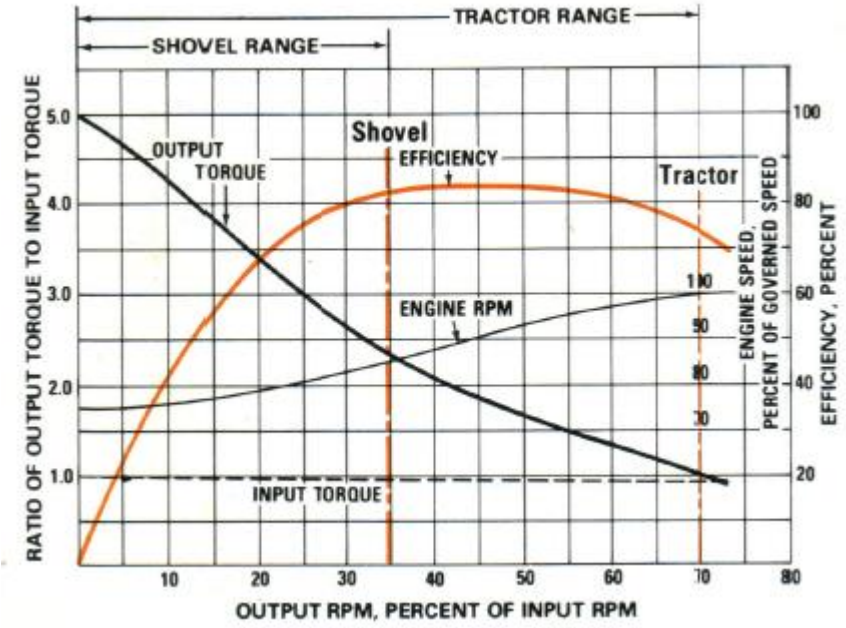

Table 1 shows a typical torque converter efficiency vs rpm curve (JM clutches and converters). Most modern torque converters have a lock up clutch which lock the turbine and impellor together when they are at similar speeds or coupling point. This would only occur during cruising conditions. Under these conditions there is no slip and therefore 100% transfer of power and no heat generated other than due to component friction.

Most driving situations are not cruising and the torque convertor clutch is most often disengaged. The results of this slip is heat generated into the transmission fluid. How much heat depends on how much slip and turbulence is occurring during a specific driving situation. Some of the factors that affect the amount of heat generated, include towing, driving speed, climbing steep mountains or hills, wind effect and weight being carried. Overheating is the number one cause of failure in automatic transmissions so controlling this heat generation is very critical to the life of the transmission. A general figure of 15% average power loss through a torque converter is considered reasonable on current model vehicles. There are promising developments to reduce this heat loss to a negligible level rather than recycle the wasted thermal energy produced. A thermal generator using the wasted heat from a torque converter may only have an application as an aftermarket kit on an older type less efficient torque converter.

Older type automatic transmissions were only 3 speed units and relied on the slip of the torque converter to smoothen out the big jump between the gear ratios. Modern day automatic transmissions have numerous gear ratio with 8 gears now standard on BMW and many other cars (ZF8HP). The closer the gear ratios, the less the need for torque converter slip. Torque converter designs are now moving towards being used to simply replace the conventional clutch. The torque converter will get the vehicle moving and the lock up clutch will engage shortly after that. The following is predicted by Middelman and Wagner (2010) of the Schaeffler group in there paper ‘Torque converters as a system’.

- Number of gear ratios of automatic transmissions will continue to increase.
- Duty cycle of an unlocked torque converter will decrease further.

Additionally engine designs are moving to higher torque, lower rotational speeds and reduced number of cylinders in the never ending drive to improve fuel consumption. This results in higher torsional vibration excitation due to lower number of cylinders coupled with lower excitation frequencies. Higher turbocharging pressures with corresponding torque increase also lead to increased excitation amplitudes (Faust H, 2014). These factors lead to an increased dampening requirements on the torque convertor and lock up clutch assembly. Centrifugal pendulum type absorbers running in oil have been developed in recent years and facilitate early lock up even at very low engine speed (Faust H, 2014)

Thermal waste in torque converters could be reduced to a negligible level as the above mentioned technologies continue to improve.

2.1.3 Braking systems

When we purchase fuel for our vehicles we are effectively purchasing the heat that that fuel can produce. In other words the calorific value of the fuel is what is actually potentially useful to us. If we consider the calorific value of a fuel as 45 MJ/kg and lose 75% of that energy to the exhaust system, cooling system and driveline. This leaves us with 11.25 MJ/kg of heat energy that we have actually managed to convert into kinetic energy. This kinetic energy of the vehicle has been achieved by expensive complex components, and a process which is inherently inefficient. After all this hard work and effort to get the vehicle moving, if the we suddenly need to stop then a conventional braking system simply converts this hard earned kinetic energy back to heat. Obviously this is a fairly wasteful process and any form of recovery of this wasted energy would be beneficial.

Heat is a degraded form of energy and it is more difficult to convert to other forms of energy without large losses. Mechanical and electrical energy are “noble” forms of energy and it is theoretically possible to transfer one into the other without loss (Da Rosa, Aldo V, 2012, pp 92). Any braking system energy recovery system would therefore be much more efficient if it could convert the mechanical kinetic energy directly into electrical energy or another form of mechanical potential energy without having to go through any heat transfer process. In recent years many vehicle manufacturers have made commercially available regenerative braking systems for their vehicles. Development of this technology continues at a steady rate and regenerative braking systems could be standard features on vehicles shortly.

2.2 Thermodynamic fundamentals and energy quality

The first law of thermodynamics is simply a statement that energy cannot be created or destroyed but only transformed from one form to another. This conservation of energy principle is used extensively in all area of engineering and physics and not just thermodynamics. The first law of thermodynamic does not fully describe the physical world of heat and energy on its own. For example if we were to allow a cup of hot coffee to cool in a room, after a certain time period the coffee would be at the same temperature as the room. The overall energy of the coffee would be less and the overall energy of the room would be more. This process cannot occur in reverse unless some form of work is done to make the heat flow from the room into the cup of coffee. The energy

available to do useful work is also of a lesser quality even though the quantity is the same. Hence the second law of thermodynamic which states that processes occur in a certain directions and that energy has quality as well as quantity. This introduces the concept that not all energy transformation processes are reversible. Heat can only flow in the direction of the temperature gradient unless work is done to reverse the flow. The quality of energy is also degraded as the energy transformation process occurs. Quantity of energy is always conserved but the quality of energy is not. Wasting energy is really the process of allowing energy to change to a less useful form without getting any work done. High quality thermal energy at high temperature has high work output potential and is more desirable than an abundance of low temp thermal energy. No thermodynamic process can occur unless it satisfies both the first and second law of thermodynamics.

Converting work into varies forms of energy is generally easily done, however converting varies forms of energy into work is often not as easy and particularly so for heat energy. For example it is possible to convert 100% of work energy into heat energy but the reverse is not possible. Heat engines of varies types are designed to convert heat energy into work. Although the operating principles and cycles may be different from one heat engine to the next, all heat engines receive heat from a high temperature source and convert part of this heat into work. The remaining waste heat is rejected to a low temperature sink. A portion of the work output of a heat engine is consumed internally to maintain a continuous cycle of operation (Cengel, Boles, 2002, pp 249).

The second law of thermodynamics can be expressed in varies statements. One of which is the Kelvin-Planck statement which states, "*It is impossible for any device that operates on a cycle to receive heat from a single reservoir and produce a net output of work".* Heat engines that operate on a continuous cycle must exchange heat with a high temperature source and a low temperature sink. As a result of these physical limitations no heat engine can have a thermal efficiency of 100%, it is a necessary part of their operation that heat is always rejected to the environment.

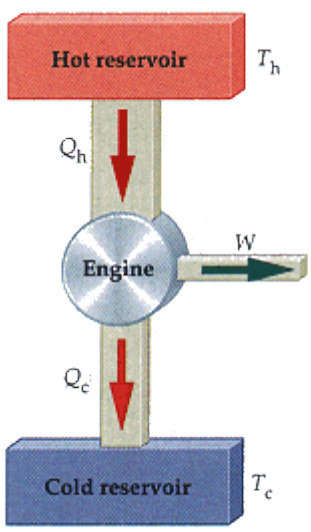

Figure 1 Heat flow diagram (http://user.physics)

The percentage of the overall heat energy supplied to a heat engine that gets converted to useful work is termed the thermal efficiency of the engine.

2.1

$$\boldsymbol{Performance = \frac{Desired\ output}{Required\ input}}$$

2.2

$$\boldsymbol{Thermal\ efficiency = \frac{Net\ work\ output}{Total\ heat\ input}}$$

Letting

Qin = amount of heat absorbed during combustion (kJ).

$Qout$ = amount of heat rejected (kJ).

$Wout$ = work output (power output) (kJ).

$Wnet$ = work input required to complete cycle (compression) (kJ)

and

2.3

$$\boldsymbol{Wnet = Wout - Win} \quad \text{kJ}$$

then

2.4

$$\boldsymbol{Thermal\ efficiency = \frac{Wnet}{Qin}}$$

2.3 Thermal efficiency of internal combustion engines

Heat engines operate on cycles where work is done on the working fluid during part of the cycle and work is done by the fluid in another part of the cycle. The difference between the two being the net work output ($Wnet$ equation 2.3). The cycle efficiency is maximised by having processes that require the least amount of Win and the maximum amount of $Wout$. Theoretically this could be achieved by having an engine that operates completely on reversible cycles. Reversible processes cannot be achieved in practice but only form a basis to establish a maximum possible theoretical upper limit with which to compare real engines.

2.3.1 Carnot efficiency

The Carnot cycle is a completely reversible cycle first proposed by French engineer Sadi Carnot in 1824. The cycle consists of four reversible engine cycles two of which are adiabatic and the other two isothermal.

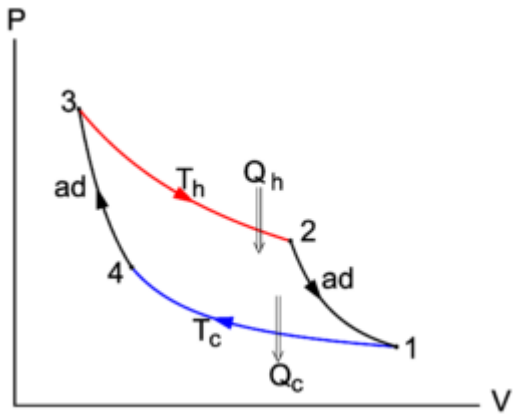

Figure 2 Carnot engine cycle (http://hyperphysics)

The first process (1-4) begins with the isothermal compression (compression at constant temperature). During this stage heat is rejected from the working fluid as the fluid is compressed and work is done on the fluid. The second process (4-3) is adiabatic compression (no heat is allowed to leave the fluid) and the fluid temperature increases from Tc to Th. During process three (3-2) heat is added to the fluid and expansion occurs in an isothermal manner. Work is done by the fluid due to the heat addition. During process four (2-1) heat addition stops and expansion occurs in an adiabatic manner until temperature Tc is reached.

The end result is the pressure – volume (P-V) diagram show in figure 2. The work done by the cycle is the area enclosed by the four processes. The efficiency of the Carnot engine is therefore the maximum that a heat engine can achieve when operating between set temperature limits Th and Tc.

2.5

$$\boldsymbol{Carnot\ efficiency = 1 - \frac{Tc}{Th}}$$

As can be seen from the Carnot equation (2.5) that the only variables that effect the efficiency are the upper and lower temperature limits. The efficiency is improved the greater the temperature difference between the heat source and the heat sink. This highlights the point made earlier regarding energy quality. The lower the temperature of the hot sources for the same cold sources temperature results in lower maximum possible thermal efficiency and therefore less energy quality.

2.3.2 Otto cycle

The Carnot engine cycle represents the maximum efficiency that can be achieved by a heat engine. However this engine cycle has no real practical application as the cycle is extremely slow to complete. Other engine cycles, such as the Otto cycle, are of more practical value even though they cannot achieve the same theoretical efficiency limits of the Carnot cycle.

The Otto cycle is the ideal cycle for a petrol fuelled reciprocating piston engine. The cycle was first proposed by Beau de Rochas in 1862. Nikolaus A. Otto successfully built the first conventional four stroke petrol engine in 1876 based on this cycle. In practical operation engine cycles are very complex to evaluate. To reduce the analysis to a manageable level, the following approximations are made, commonly known as air-standard assumptions:

- The working fluid is air, which continuously circulates in a closed loop.
- The air behaves as an ideal gas.
- All processes in the cycle are internally reversible.
- The combustion process is idealised as a heat addition process from an external source.
- The exhaust process is replaced by a heat rejection process that restores the working air to the original temperature.

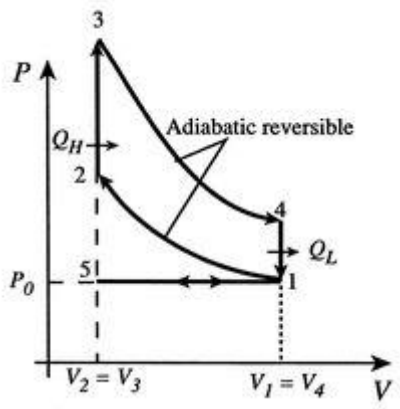

Figure 3 Idea Otto engine cycle (http://web.mit.edu)

The first stroke (1-2) is the compression stroke where the piston moves from bottom dead centre (BDC) and volume V_1 to top dead centre (TDC) and V_2. During this stroke the air is compressed in an adiabatic and completely reversible manner (isentropic). Work is done on the working fluid to achieve this compression. When piston is at V_2 heat is added to the fluid with negligible change in volume (2-3). This simulate the combustion of a spark-ignition engine very closely as combustion occurs very quickly with the piston not getting much time to move past TDC. This point in the cycle is also called the ignition point. The second stroke (3-4) occurs as the piston move back from V_3 to V_4. This is termed the power stroke and work is done on the surroundings by the working fluid as the fluid expands in an isentropic manner pushing the piston back down the bore to V_4. The piston is now back where it started at bottom dead centre. At point 4 heat is released from the working fluid which reduces the pressure back to the original pressure at point 1. This process simulate the

exhaust valve opening and releasing the relatively high pressure and hot exhaust gases to atmosphere through the exhaust pipe. The next two stoke of the piston are only necessary only for cylinder filling and scavenging. The exhaust stroke (1-5) occurs as the piston moves up the bore with the exhaust valve open pushing the exhaust gases out. The intake stroke (5-1) occurs as the piston moves back down the bore with the inlet valve open and allowing a fresh charge of air/fuel mixture into the engine. The work done during the cycle is the area enclosed in figure 3 by the process 1-2, 2-3, 3-4 and 4-1.

Given:

2.6

$$\boldsymbol{Q_{in} = C_v(T_3 - T_2)}$$

And

2.7

$$\boldsymbol{Q_{out} = C_v(T_4 - T_1)}$$

And

2.8

$$\boldsymbol{\frac{T_1}{T_2} = (\frac{V_2}{V_1})^{k-1}}$$

Where C_v is the specific heat capacity of air at 25℃ at constant volume, and C_p is the specific heat capacity of air at 25 ℃ at constant pressure. k is the ratio of specific heat capacities $\frac{C_p}{C_v}$.

2.9

$$\boldsymbol{Thermal\ efficiency\ (Otto) = \frac{Wnet}{Qin}}$$

2.10

$$\boldsymbol{Thermal\ efficiency\ (Otto) = 1 - \frac{T_4 - T_1}{T_3 - T_2}}$$

2.11

$$\boldsymbol{Thermal\ efficiency\ (Otto) = 1 - \frac{1}{(\frac{V_1}{V_2})^{k-1}}}$$

Letting $\frac{V_1}{V_2}$ equal compression ratio (r)

Then

2.12

$$\boldsymbol{Thermal\ efficiency\ (Otto) = 1 - \frac{1}{(r)^{k-1}}}$$

Equation 2.12 shows that the thermal efficiency of an Otto cycle engine depends on the compression ratio (r) of the engine and the specific heat ratio of the working fluids (k). The higher the compression ratio and the value of k the greater the efficiency. In practical engines air is used as the working fluid so the value of k is set to that of air. The compression ratio (r) can be increased to improve the efficiency and therefore the power output however the compression ratio is also limited by the auto ignition point of the air-fuel mixture. A compression ratio of 12:1 will produce a theoretical maximum efficiency of 63%. This is the maximum possible efficiency that can be achieved by an Otto cycle engine with a compression ratio of 12:1. This efficiency is well below that of the Carnot engine cycle which is based on the difference in temperature between the T_3 and T_1.

The Otto cycle thermal efficiency of 63% with a compression ratio 12:1 represents the maximum possible efficiency for this engine under absolutely perfect idealised conditions. It can never be achieved in the real world. It does however give a theoretical target with which to compare real engines. Even if 63% thermal efficiency were achieved this would still mean that 37% of our initial input heat energy would have to be discharged to the environment as thermal waste.

We conclude that every heat engine must waste some heat energy ($Qout$) by transferring it to a low temperature heat sink in order to compete the engine cycle (figure1). The quality of this rejected heat energy is also of a lower value due to it being at a much lower temperature. This thermal energy is a necessary waste product of our engine cycle. It is important to note that the heat rejected by an engines radiator is heat generated from component and material inefficiencies. The heat rejected by the exhaust system is the thermal waste that is necessary to complete the engine cycle.

Up until recent times we have chosen to ignore this thermal waste. However as energy usage and conservation becomes more and more critical it become obvious that ignoring such a large quantity of low quality thermal energy may be very foolish. Many areas of human activity are very good at recycling waste products and others not so much. For example consider cattle going to the abattoir. Not all of the meat product will find its way to the supermarket and the butcher (high quality). A large portion of the resource being the bones, blood and so forth (low quality).In times of abundant supply may have been discarded. Nowadays through innovation and drive for maximum profits very little of the initial resource is discarded as waste. Why should this not be the same for our thermal energy supplies?

Table 2 Efficiency vs compression ratio curve for Otto cycle engine (http://home.iitk.ac).

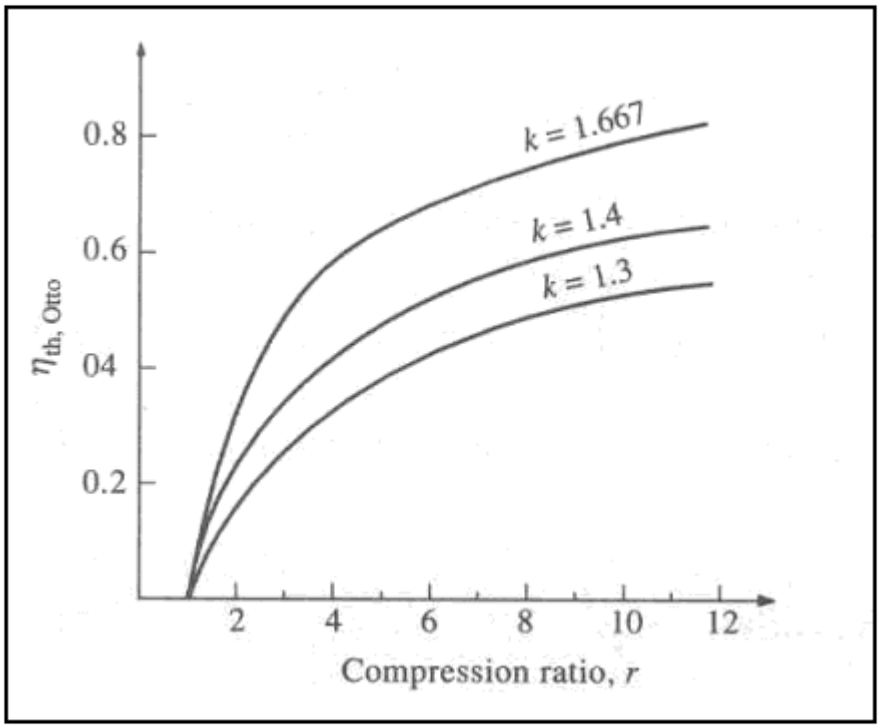

Chapter 3

Thermoelectric technology

3.1 Introduction

Thermoelectric technology is the study of devices that can convert thermal energy directly into electric energy or visa versa. In 1821 Thomas J.Seebeck discovered that an electromotive force could be generated from a circuit of two dissimilar wires when one of the junctions were heated as shown in Figure 4. This is called the Seebeck effect. This principle, also called a thermocouple, is used extensively in temperature sensor technology.

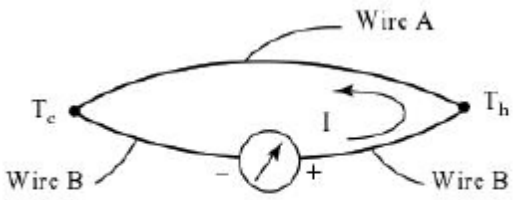

Figure 4 Thermocouple (Lee, Ho Sung, 2010)

The potential difference produced across the junction is proportional to the temperature difference between the hot (T_h) and cold (T_c) junctions.

3.1

$$\boldsymbol{V = \alpha \Delta T}$$

Where $\Delta T = T_h - T_c$ and α is called the Seebeck coefficient or thermopower.

While Seebeck was the first to notice the Seebeck effect much work was done at a later stage by Jean Peltier and William Thomson to define the physics of thermoelectricity. Thermoelectric effects consist of three effects: Seebeck effect, Peltier effect and the Thomson effect. Although the principles were developed in the mid to late nineteenth century, the efficiencies were very low and not much interest was shown in this technology as an energy conversion technique, until recent developments in nanotechnology. Despite low thermal efficiencies (typically around 5%) (Rowe and Min 1998, pp. 193-8) thermoelectric devices have no moving part and therefore inherently more

reliable than any other heat to electric conversion techniques. This high reliability has seen favorable applications in areas such as industrial instrumentation, military, medical, aerospace and portable or remote power generation.

In recent years with increasing concern regarding environmental issues, extensive research into nonconventional technologies of converting heat into electricity have been accelerated. Thermoelectric power generation has emerged as a promising technology to this end. Particularly in the area of converting low quality waste heat energy directly into electricity. When the heat energy used to drive a thermal generator is wasted or readily available, it is in fact free. The fact that the energy conversion process efficiency is very low becomes less of an issue. If the fuel/heat source were very expensive then this low efficiency process would not be ideal. These factors make thermal generation an ideal process for converting the unavoidable waste thermal energy from a heat engine into electricity or even another fuel source to be consumed by the engine, thereby increasing the overall efficiency of the engine cycle.

3.2 Thermoelectric Generator (TEG)

A thermoelectric generator is a power generator without moving parts. It is silent in operation and relatively reliable. The thermoelectric module consists of p-type and n-type semiconductor materials connected as shown in Figure 5. The semiconductor elements are connected thermally in parallel and electrically in series. The p and n elements may be of similar or dissimilar materials. The performance of thermoelectric devices is measured by a figure of merit (Z) for which the units are 1/℃.

3.2

$$\boldsymbol{Z = \frac{\alpha^2}{\rho k}}$$

where α = Seebeck coefficient, $V/℃$

ρ = electrical resistivity, Ohm.cm

k = thermal conductivity, W/cm.℃

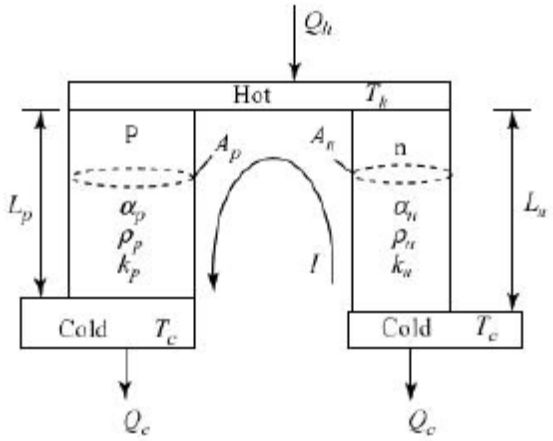

Figure 5 Thermoelectric couple with dissimilar p and n elements (Lee, Ho Sung, 2010)

A high figure of merit (Z) is desirable for high performance and efficiency. A high Seebeck coefficient, low thermal conductivity and low electrical resistivity are needed to achieve this. Reducing thermal conductivity will not benefit the heat flow through the materials therefore it is preferable to rather reduce electrical resistivity as much as possible and maximize the Seebeck coefficient. Table 3 show some values of the figure of merit (Z) for some popular semiconductor materials. Bithmuth telluride (Bi_2Te_3) and its alloys are widely used for thermoelectric cooling (TEC), while Lead telluride ($PbTe$) is commonly used for thermoelectric generators (TEG) (Lee, Ho Sung, 2010, pp 105). A dimensionless figure of merit (ZT_{ave}) is also commonly used with T_{ave} being the average temperature of the hot and cold junction.

Table 3 Figures of merit for common semiconductor materials (Lee, Ho Sung, 2010)

Material	Type	Temperature (°C)	Figure of merit $Z\,(K^{-1})$	Source
Bi_2Te_3	p	25	2.5×10^{-3}	[4]
Bi_2Te_3	n	25	2.5×10^{-3}	[4]
SbBiTeSe	p	70	3.0×10^{-3}	[5]
Bi SbTe	p	150	2.5×10^{-3}	[5]
Bi_2Te_3-74Sb_2Te_3	n	150	3.0×10^{-3}	[6]
Bi_2Te_3-25Bi_2Se_3	p	150	2.7×10^{-3}	[6]
PbTe	n, p	450 (325–625)	1.3×10^{-3}	[9]
ZnSb	p	175	1.4×10^{-3}	[4]
SiGe	p	1,000	0.4×10^{-3}	[1]
SiGe	n	1,000	0.8×10^{-3}	[1]
GeTe	p	450	1.7×10^{-3}	[4]
MnTe	p	900	0.4×10^{-3}	[4]
$CeS_{1.4}$	n	1,100	1.8×10^{-3}	[4]
$AgSbTe_2$	p	400	1.3×10^{-3}	[4]
InAs	n	700	0.7×10^{-3}	[4]

The p and n junction as shown in Figure 5 can be manufactured of similar or dissimilar materials. It is customary to use similar materials on a particular thermocouple, however most commercially available thermocouples are of dissimilar materials in an effort to maximize the figure of merit (Z) (Lee, Ho Sung, 2010, pp. 106).

Value of Seebeck coefficient (α), electrical resistivity (ρ) and thermal conductivity (k) for the combined p and n semiconductor material are obtained as follow

3.3. a

$$\boldsymbol{\alpha = \overline{\alpha_p} - \overline{\alpha_n}}$$

3.3 b

$$\boldsymbol{\rho = \overline{\rho_p} + \overline{\rho_n}}$$

3.3 c

$$\boldsymbol{k = \overline{k_p} + \overline{k_n}}$$

For similar materials

3.4 a

$$\boldsymbol{\alpha_p \approx \alpha_n}$$

3.4 b

$$\boldsymbol{\rho_p \approx \rho_n}$$

3.4 b

$$\boldsymbol{k_p \approx k_n}$$

For dissimilar materials the material figure of merit (Z) for an optimum geometry is calculated using the following equations. For similar materials equation 3.2 applies.

3.5

$$\boldsymbol{Z = \frac{(\alpha_p - \alpha_n)^2}{\left[(k_p \rho_p)^{\frac{1}{2}} + (k_n \rho_n)^{\frac{1}{2}}\right]^2}}$$

or

3.5 a

$$\boldsymbol{Z = \frac{(\alpha_p - \alpha_n)^2}{KR}}$$

where

3.5 b

$$\boldsymbol{KR} = \left[\left(\boldsymbol{k_p\rho_p}\right)^{\frac{1}{2}} + \left(\boldsymbol{k_n\rho_n}\right)^{\frac{1}{2}}\right]^{\boldsymbol{2}}$$

Where R is the overall internal electrical resistance of the p and n elements and K is the overall thermal conductance.

3.5 c

$$\boldsymbol{K} = \frac{\boldsymbol{kA}}{\boldsymbol{L}}$$

And for dissimilar materials

3.5 d

$$\boldsymbol{K} = \frac{\boldsymbol{k_pA_p}}{\boldsymbol{L_p}} + \frac{\boldsymbol{k_nA_n}}{\boldsymbol{L_n}}$$

3.5 e

$$\boldsymbol{R} = \frac{\boldsymbol{\rho L}}{\boldsymbol{A}}$$

3.5 d

$$\boldsymbol{R} = \frac{\boldsymbol{\rho_pL_p}}{\boldsymbol{A_p}} + \frac{\boldsymbol{\rho_nL_n}}{\boldsymbol{A_n}}$$

For optimum geometry the following relationships apply.

3.5 c

$$\boldsymbol{KR} = \left(\frac{\boldsymbol{k_pA_p}}{\boldsymbol{L_p}} + \frac{\boldsymbol{k_nA_n}}{\boldsymbol{L_n}}\right)\left(\frac{\boldsymbol{\rho_pL_p}}{\boldsymbol{A_p}} + \frac{\boldsymbol{\rho_nL_n}}{\boldsymbol{A_n}}\right)$$

And

3.5 d

$$\frac{\boldsymbol{L_n/A_n}}{\boldsymbol{L_p/A_p}} = \left(\frac{\boldsymbol{\rho_pk_n}}{\boldsymbol{\rho_nk_p}}\right)^{\frac{1}{2}}$$

3.2.1 Conversion efficiency

Equations 3.5 and 3.5d are useful in the design of thermoelectric coupling for both the selection of materials to maximize Z and obtain the optimum geometries of the dissimilar p and n junction semiconductor material (Lee, Ho Sung, 2010, pp. 106). Similar materials have the same base material and therefore the same geometries in the p and n junctions. The analysis is simplified as $L_p = L_n$ and $A_p = A_n$. Additionally the heat flow into the hot junction is made up of three components: the heat associated with the Seebeck effect, the half of joule heating and thermal conduction. As a result the heat flow into the hot junction is defined by equation 3.6.

3.6

$$\boldsymbol{Q_h = \alpha T_h I - 0.5 I^2 R + K(T_h + T_c)}$$

Where I is the current flow through the hot junction as shown in Figure 6. The power generated across the load is given by:

3.6 a

$$\boldsymbol{W = I^2 R_L}$$

The conversion efficiency of the thermal generator is given by:

3.6 b

$$\eta_t = \frac{\boldsymbol{W}}{\boldsymbol{Q_h}}$$

Heat rejected at cold junction from first law of thermodynamics:

3.6 c

$$\boldsymbol{Q_c = Q_h - W}$$

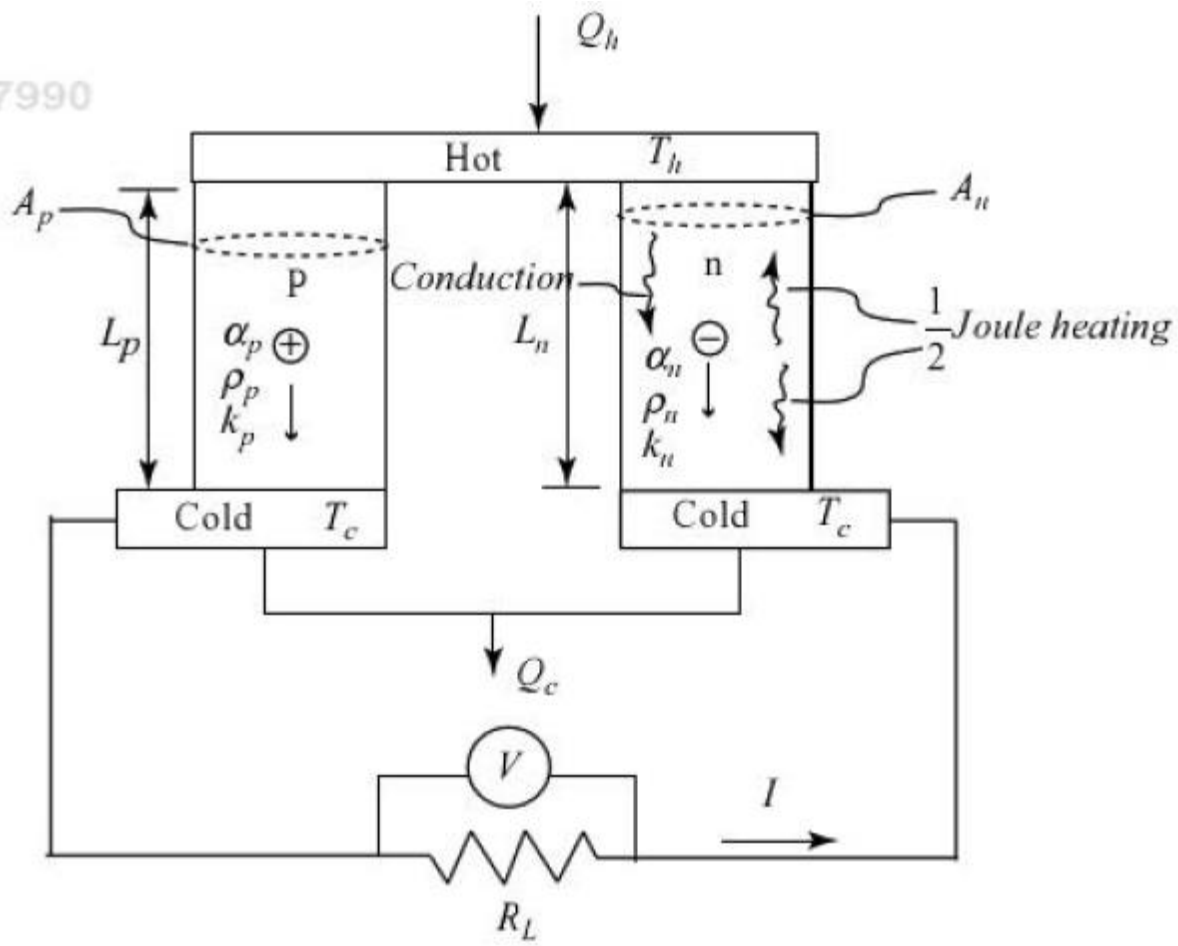

Figure 6 Thermoelectric generator (Lee, Ho Sung, 2010)

The open circuit voltage is given by Ohms law:

3.7

$$\boldsymbol{V_{oc} = I(R_L + R)}$$

and equation 3.1

$$\boldsymbol{V = \alpha \Delta T}$$

Combining equation 3.7 and 3.1 to obtain an equation for the current flow (I).

3.7 a

$$\boldsymbol{I = \frac{\alpha \Delta T}{(R_L + R)}}$$

The conversion efficiency of equation 3.6b can be rewritten in the form of:

3.8

$$\eta_t = \frac{\frac{R_L}{R}\left(1 - \frac{T_c}{T_h}\right)}{\left(1 + \frac{R_L}{R}\right) - 0.5\left(1 - \frac{T_c}{T_h}\right) + \frac{1}{2Z\bar{T}}\left(1 + \frac{R_L}{R}\right)^2\left(1 + \frac{T_c}{T_h}\right)}$$

From equation 3.8 it can be seen that the conversion efficiency is a function of three dimensionless values namely R_L/R, $Z\bar{T}$ and T_c/T_h. To obtain the maximum conversion efficiency, equation 3.8 is differentiated with respect to R_L/R, and the derivative set to zero. This yields the optimum R_L/R ratio for **maximum conversion efficiency**.

3.8 a

$$\frac{R_L}{R} = (1 + Z\bar{T})^{\frac{1}{2}}$$

Similarly differentiating power equation 3.6a with respect to R_L/R and setting the derivative to zero yield the R_L/R ratio of 1 for **maximum power conversion**.

3.8 b

$$R_L = R$$

Substituting these valves back into the equation 3.8 yield an equation for maximum efficiency.

3.8 c

$$\eta_{max\ efficiency} = \frac{\left(1 - \frac{T_c}{T_h}\right)(1 + Z\bar{T})^{\frac{1}{2}} - 1}{(1 + Z\bar{T})^{\frac{1}{2}} + \frac{T_c}{T_h}}$$

and maximum power

3.8 d

$$\eta_{max\ power} = \frac{\left(1 - \frac{T_c}{T_h}\right)}{\frac{2}{Z\bar{T}}\left(1 + \frac{T_c}{T_h}\right) + 2 - \frac{1}{2}\left(1 - \frac{T_c}{T_h}\right)}$$

3.2.2 Maximum performance parameters

The performance parameters ratios are the ratios of the actual performance compared the maximum performance. These values are important in thermocouple design and component selection. The values of obvious interest are power, volt and amps. It can also be noted from equation 3.8 that the only externally controllable dimension is the R_L/R ratio. The other two dimensions being the Z value and the temperature of the hot and cold junction. The Z value being a function of the semiconductor material and the temperature gradient being set by the external environment. The performance of thermoelectric generators is therefore heavily dependent on the load resistance (R_L), the internal resistance (R) being a property of the semiconductor material and the module geometry. The performance parameters of power, voltage and amps are plotted in Table 4. The value of $Z\bar{T}$ and T_c/T_h in equation 3.8 being set to 1 and 0.5 respectively.

Maximum power ratio with $Z\bar{T}$ = 1 and T_c/T_h = 0.5

3.9

$$\frac{\boldsymbol{W}}{\boldsymbol{W_{max}}} = \frac{\boldsymbol{4\frac{R_L}{R}}}{\boldsymbol{\left(\frac{R_L}{R}+1\right)^2}}$$

Maximum current ratio with $Z\bar{T}$ = 1 and T_c/T_h = 0.5

3.9 a

$$\frac{\boldsymbol{I}}{\boldsymbol{I_{max}}} = \frac{\boldsymbol{1}}{\boldsymbol{\frac{R_L}{R}+1}}$$

Maximum current ratio with $Z\bar{T}$ = 1 and T_c/T_h = 0.5

3.9 b

$$\frac{\boldsymbol{V}}{\boldsymbol{V_{max}}} = \frac{\boldsymbol{\frac{R_L}{R}}}{\boldsymbol{\frac{R_L}{R}+1}}$$

Table 4 TEG characteristics chart with $Z\bar{T}$ = 1 and T_c/T_h = 0.5 (Lee, Ho Sung, 2010).

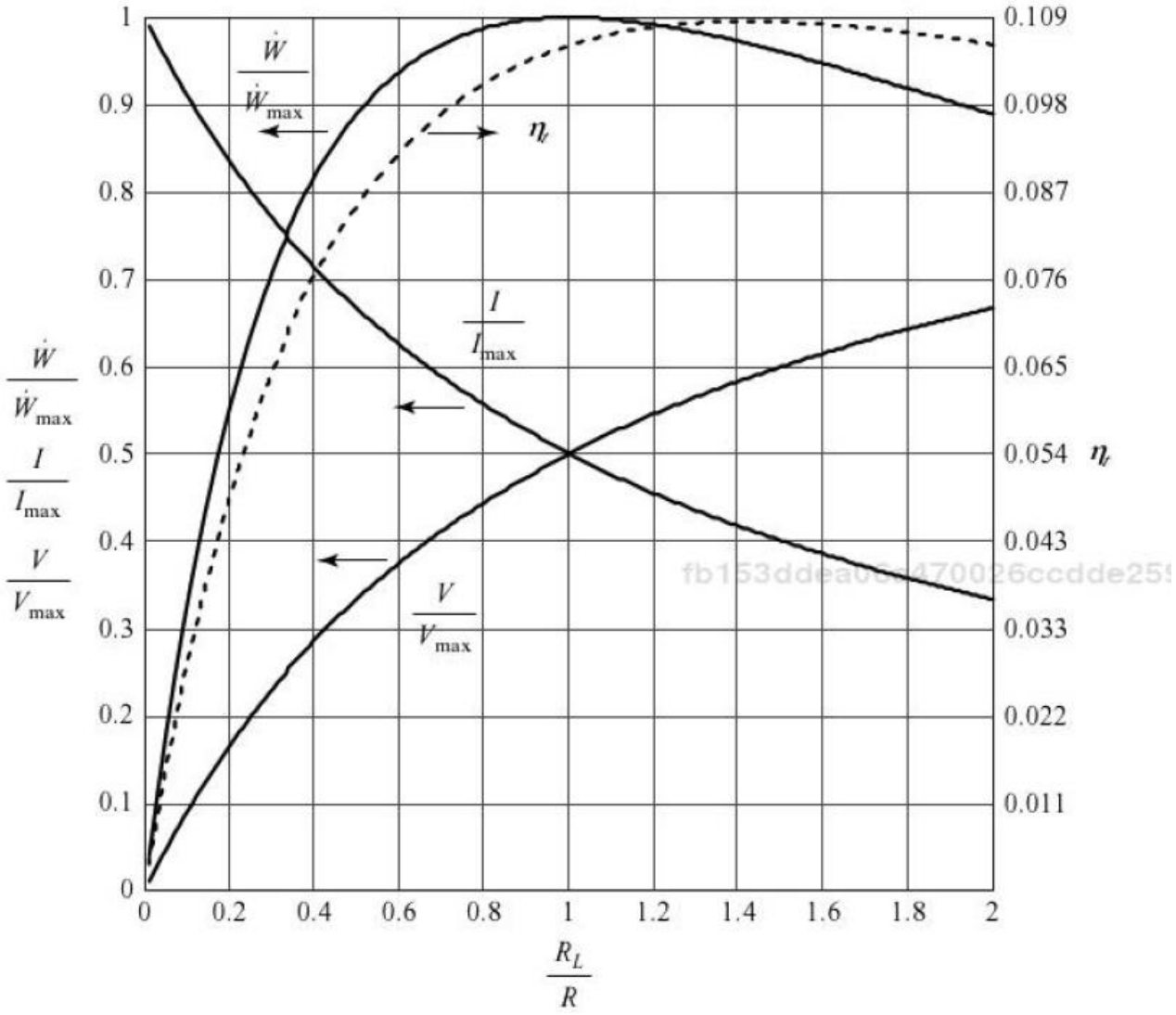

As shown in Table 4 the performance of thermoelectric generators vary greatly with load resistance. It is therefore critical to arrange the load resistance sensibly to achieve optimum performance. Optimum performance can be considered to be between maximum power and maximum conversion efficiency points. In the case of Table 4 this would mean a R_L/R ratio between 1 and 1.414.

Some interesting observation from Table 4 are that the maximum power occurs at R_L/R = 1. This is exactly as predicted by equation 3.8b. This is also the point at which the V/V_{max} and the I/I_{max} curves intersect. Table 5 shows the variation in the maximum conversion efficiency point and maximum power conversion point as a function of $Z\bar{T}$ and T_c/T_h For low values of $Z\bar{T}$ the variation is very small and may be neglected especially when $Z\bar{T} \approx 1$. Maximum power may be considered as maximum performance under these conditions. However for $Z\bar{T} \geq 3$ then the discrepancy becomes significant and needs to be considered in the design.

Table 5 Maximum conversion efficiency and maximum power efficiency (Lee, Ho Sung, 2010).

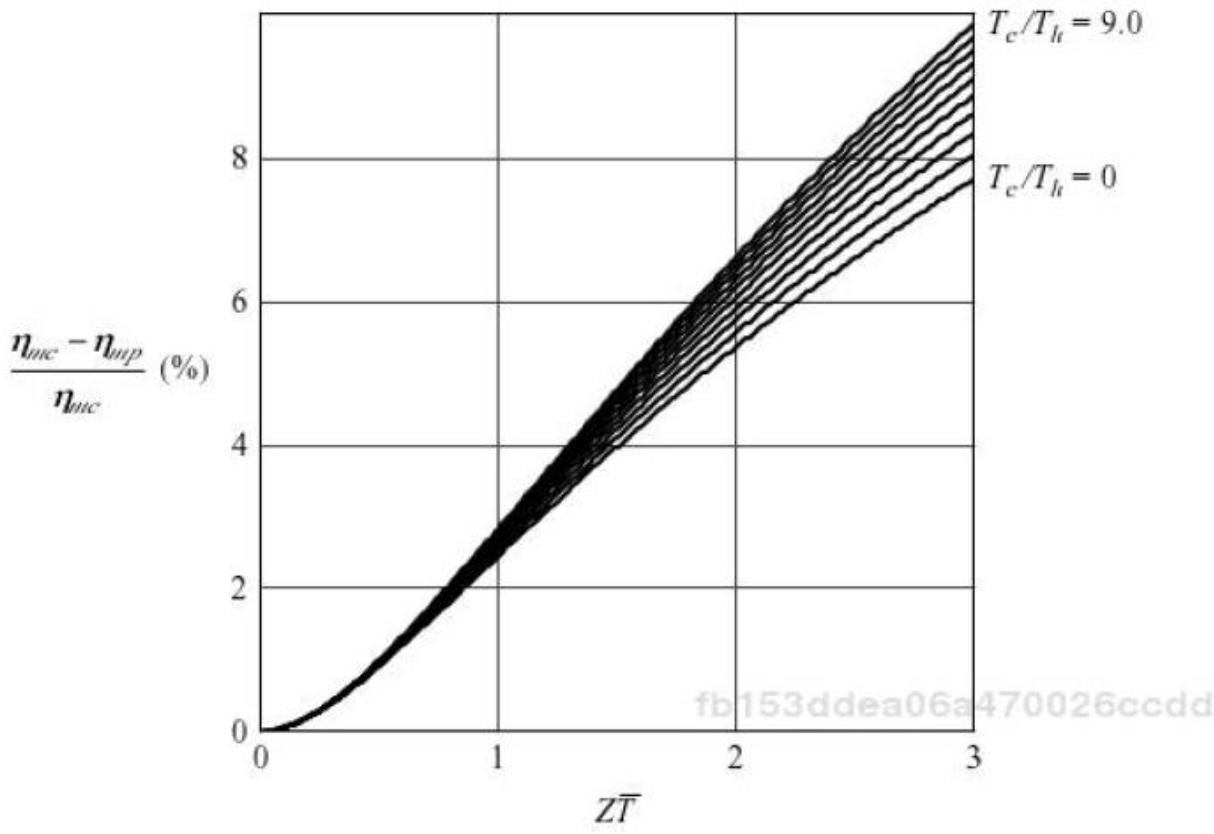

3.2.3 Thermal and Electrical contact resistances for TEG

In the design of real thermoelectric devices consideration must be made for the thermal and electrical resistances of the component junctions.

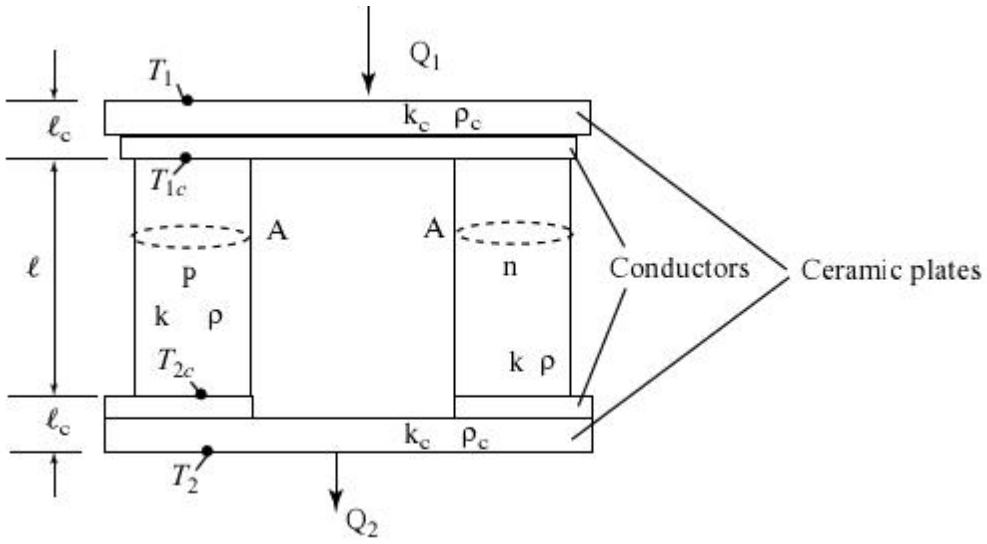

Figure 7 Configuration of a real thermoelectric couple (Lee, Ho Sung, 2010)

Figure 7 shows the configuration of a practical thermoelectric couple where n-type and p-type thermoelements are connected in series by highly conductive metal strips. The thermocouples are connected electrically in series and thermally in parallel between thermally conducting but electrically insulating ceramic plates. In the equations presented so far the electrical and thermal resistances have been neglected as they are relatively small. However in the design and selection of practical thermoelectric generator (TEG) they would need to be considered.

The following is an overview of the equations used and basic derivation. The equations used are as presented by Lee Ho Sung 2010.

Heat flowing in the hot junction is given by:

3.10

$$\boldsymbol{Q_1 = \frac{Ak_c}{l_c}(T_1 - T_{1c})}$$

and

3.11

$$\boldsymbol{Q_1 = \alpha I T_{1c} - \frac{1}{2}I^2R + \frac{Ak}{l}(T_{1c} - T_{2c})}$$

Heat flowing out of cold junction is given by:

3.12

$$\boldsymbol{Q_2 = \frac{Ak_c}{l_c}(T_{2c} - T_2)}$$

and

3.13

$$\boldsymbol{Q_2 = \alpha I T_{2c} - \frac{1}{2}I^2R + \frac{Ak}{l}(T_{1c} - T_{2c})}$$

where

$\alpha = \alpha_p - \alpha_n$ Seebeck coefficient of thermoelements.

$k = k_p + k_n$ Thermal conductivity of the thermoelements.

k_c is the thermal contact conductivity of both the ceramic plates and the contact thermal contacts.

l is the thermoelement length.

l_c is the thickness of the contact layer.

The overall electrical resistance of a thermocouple (R) is made up of the resistance of the thermocouple material $(R_{m)}$ and the resistance over the electrical strip and contacts$(R_{c)}$.

3.14

$$\boldsymbol{R = R_m + R_c = \frac{\rho l}{A} + \frac{\rho_c}{A} = \frac{\rho l}{A}\left(1 + \frac{\rho_c}{\rho l}\right) = \frac{\rho l}{A}\left(1 + \frac{s}{l}\right)}$$

Therefore,

3.15

$$\boldsymbol{R = R_m\left(1 + \frac{s}{l}\right)}$$

where

$\rho = \rho_p + \rho_n$ Electrical material resistivity.

ρ_c Electrical contact resistivity.

$s = \frac{\rho_c}{\rho}$

$R = \frac{\rho l}{A}$

By substituting equations 3.10 to 3.15 into each other and applying appropriate algebra a relationship is developed between the real and ideal temperature differences (Lee, Ho Sung, 2010, pp. 154). Additionally maximum power $(R_l = R)$ is assumed which produces an equation for current(I), power (W_n) and volts (V_n) in terms of real temperature and thermal/electrical resistance.

3.16

$$\boldsymbol{I = \frac{A\alpha(T_1 - T_2)}{2\rho l\left(1 + \frac{s}{l}\right)\left(1 + 3r\frac{l_c}{l}\right)}}$$

where

$r = \frac{k}{k_c}$

and

3.17

$$\boldsymbol{W_n = \frac{nA\alpha^2(T_1 - T_2)^2}{4\rho l\left(1 + \frac{s}{l}\right)\left(1 + 3r\frac{l_c}{l}\right)^2}}$$

and

3.18

$$V_n = \frac{n\alpha(T_1 - T_2)}{2\left(1 + 3r\frac{l_c}{l}\right)}$$

and

3.19

$$\eta_{real} = \frac{1 - \frac{T_2}{T_1}}{\frac{2}{ZT_{ave}}\left(1 + \frac{T_2}{T_1}\right)\left(1 + \frac{s}{l}\right)\left(1 + 3r\frac{l_c}{l}\right) + 2\left(1 + 3r\frac{l_c}{l}\right)\frac{T_{1c}}{T_1} - \frac{1}{2}\left(1 - \frac{T_2}{T_1}\right)}$$

and as $r \to 0$ and $s \to 0$ so $\eta_{real} \to \eta_{max\ power}$

3.20

$$\eta_{max\ power} = \frac{\left(1 - \frac{T_c}{T_h}\right)}{\frac{2}{Z\bar{T}}\left(1 + \frac{T_c}{T_h}\right) + 2 - \frac{1}{2}\left(1 - \frac{T_c}{T_h}\right)}$$

The effects of the thermal and electrical contact resistances are shown in Figure 8 below. As can be seen that the power output and the conversion efficiency are dependent on the thermoelement length. Long thermoelement lengths result in higher conversion efficiency where shorter thermoelements result in higher power per unit area. As a result optimal design of a particular thermoelement is a compromise between high efficiency and large power outputs. The main objectives of thermoelectric module design is to determine a set of design parameters which best meet the specifications at minimal costs.

The design theory's and equations presented so far form a useful understanding of the operation and design of a thermoelectric module. It is not practical in most situations to design a thermoelectric module specifically for a particular application. Unless of course it is intended that there are going to be a very significant number of units manufactured to offset this initial specific design cost. In most situations, especially initially, the process would be to best select what is commercially available to suit the application. For commercially available thermoelectric modules appropriate values of contact resistance are $s \sim 0.1$ and $r \sim 0.2$.

The theoretical work presented in this report based mainly on Lee, Ho Sung, 2010, Thermal design shows good agreement with the experimental work conducted by DM. Rowe, G.Min, 1998, Evaluation of thermoelectric modules for power generation (Lee, Ho Sung, 2010, pp. 157).

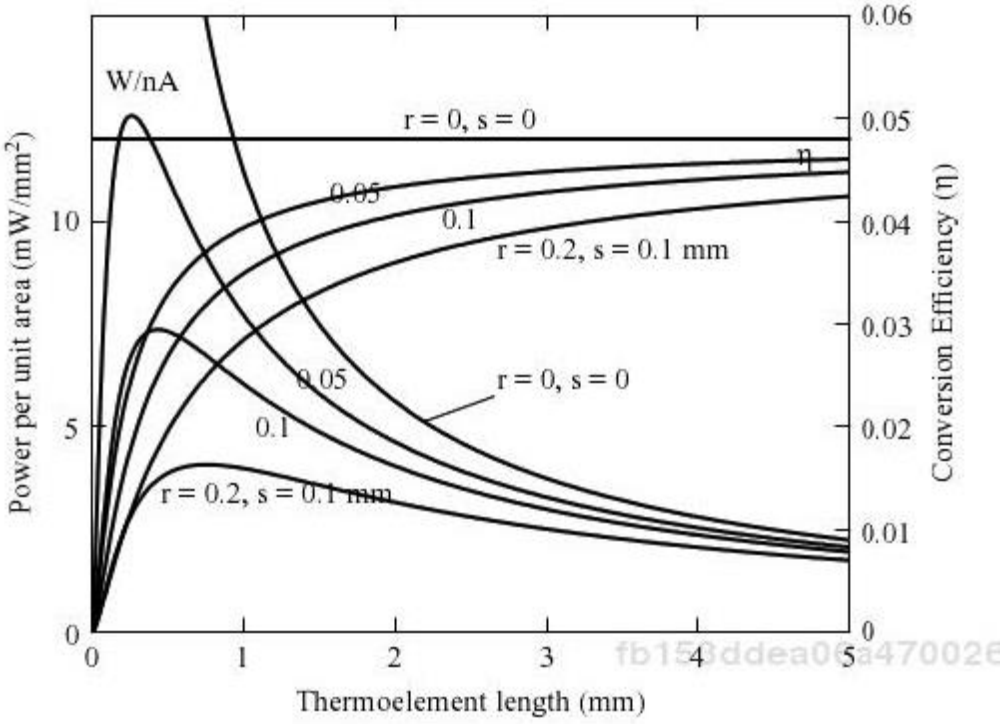

Figure 8 Power per unit area and conversion efficiency vs thermoelement length (Lee, Ho Sung, 2010)

Chapter 4

Exhaust waste heat thermal generator

4.1 Introduction

Thermal waste is an unavoidable consequence of operating a heat engine. This thermal waste can be found in the cooling system, which is a direct result of component and material inefficiencies or dumped into the exhaust system which is a requirement of operating on an engine cycle. The thermal waste is a major component of the available thermal energy. Average efficiencies of a conventional heat engine are in the range of 25 to 35%. This leaves a large amount of wasted thermal energy (75%) which is divided up approximately evenly between the exhaust system and the cooling system. Up until fairly recently this wasted thermal energy has been completely ignored because of its lower quality and potential to do further work. Thermal generator technology may not have been available or refined to a useable level to be able to use this wasted heat. Recent developments in nanotechnology have made thermal electric generators (TEG) a viable method of extracting some use out of this wasted resource. Although the efficiencies of TEG are relatively low at this stage, they appear to be hugely underutilized and it is expected that this technology will become more and more common.

This project is aiming specifically at designing a thermal generator that uses the hot exhaust gases to generate electrical power. The principles and theory used are in no way limited to hot exhaust gases. The project could have been just as easily about designing a radiator that can generate electrical power.

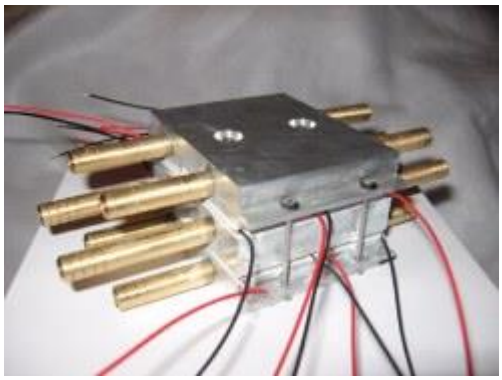

Figure 9 45 Watt liquid to liquid TEG operating on DT 115℃ (http://espressomilkcooler.com/about/)

Figure 9 shows a 45 Watt thermal generator which is commercially available and used in camping applications. Hot water flows in from a camp fire and cold water flows in the other side from a large cold source such as a water tank or a lake. As long as a temperature difference exists across the TEG then electrical power will be generated. In this case enough power is available for lighting.

4.2 Exhaust gas thermal generator

In designing a thermal generator to be placed in a modern vehicle exhaust system some factors need to be considered to ensure that the new component does not interfere with any current vehicle systems. One of the main components in a vehicle exhaust system is the catalytic convertor. A modern day catalytic convertor consists of two stages namely a reduction catalyst and an oxidation catalyst. The reduction catalyst is the first stage of the catalytic convertor and in this section the oxides of nitrogen NO_x are broken up into their core components of Oxygen $(0_{2)}$ and Nitrogen(N_2). This occurs by a reaction between Platinum, Rhodium and heat. In the second stage the unburnt hydrocarbon fuel (HC) and partially burnt carbon-monoxide(CO) are oxidized with the oxygen that was released in the first stage. Platinum, Palladium and heat are required for the second stage to complete the reaction.

The important factors to consider are that a catalytic convertor needs heat and a certain temperature range to operate efficiently. Additionally the downstream temperature of a correctly operating catalytic convertor is marginally higher than the upstream temperature due to the oxidation that occurs in the second stage. It would therefore make sense to place a thermal generator device immediately downstream of a catalytic convertor. Catalytic convertors are placed as close to the exhaust manifold as possible to ensure that they reach there operating (light up) temperature as soon as possible. These factors work in well with the fact that a thermal generator will work better the hotter the exhaust gasses are. Additional efficiency could also be achieved by heat wrapping the exhaust manifolds or treating them with some sort of ceramic coating. The aim of the wrap or coating would be to minimize the heat loss of the exhaust gasses in the engine bay prior to arrival at the catalytic convertor. This should reduce catalytic convertor warm up time and improve thermal generator ΔT. Conventional exhaust systems are designed to dissipate as much heat as possible from the exhaust gasses prior to discharging to atmosphere. In the case of an exhaust gas thermal generator this would not be the case. It would be preferred to insulate the exhaust gasses upstream of the generator and extract as much heat as possible as the gasses flow through the generator.

Insulation of the exhaust gasses as they leave the engine could potentially cause overheating problems for the catalytic convertor. Early model catalytic convertors were susceptible to overheating issues and degradation due to high temperatures and thermal cycling with time. In latter model engines the catalytic convertor is no longer the limiting factor in exhaust gas temperature control but rather the exhaust valve and exhaust port materials (McDonald and Jones, 2000). If an exhaust system were to be insulated upstream of the TEG to maximize the temperature of the exhaust gasses entering the TEG then the effects of this on the catalytic convertor needs to be carefully considered.

Figure 10 (McDonald & Jones, 2000) shows a typical exhaust gas temperature range for a petrol engine. The data presented formed part of the work by McDonald and Jones into the factors effecting the life cycle of a catalytic convertor. It can be seen that a reasonable temperature range for exhaust gas downstream of the catalytic convertor is in the range of 300℃ to 750℃.

From the above discussion the most sensible location of a TEG should be just after the catalytic convertor of an insulated up steam exhaust system. This location should minimize the heat loss in the exhaust gas and take advantage of the slight increase in exhaust gas temperature downstream

of the catalytic convertor due to the after burn effect of the oxidation section of the catalytic convertor.

If the heat exchanger units operate as efficiently as hoped and expected then the exhaust gasses could be cooled to a temperature below the boiling point of H_2O. This would mean that the latent heat of the vaporization could be utilized to enhance the efficiency of the system. H_2O, which is a major component of exhaust gasses, would no longer be discharged to atmosphere as superheated steam but as water particle and steam vapor. This may give rise to other issues related to visible emissions which would need to be considered.

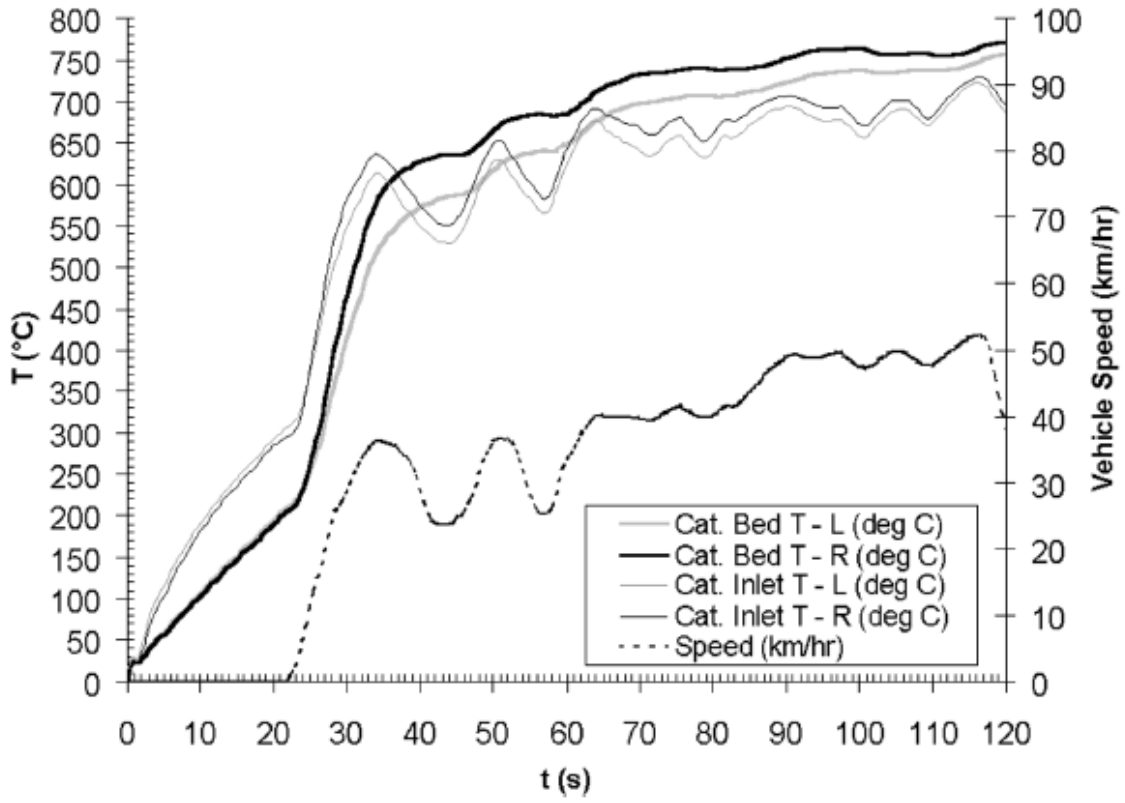

Figure 10 Exhaust gas temperature chart for Ford Explorer (McDonald & Jones, 2000)

4.2.1 TEG component selection

Thermal Electronics Corporation is a North American based company who develops, designs and manufactures thermoelectric Peltier and Seebeck effect based appliances and components. The company supplies thermoelectric components for the food, medical, commercial, and oil & gas industries. The company can supply custom designed module as well as off the shelf units The Company is also highly involved in partnering local Universities in thermoelectric research and development.

A unique new class of thermoelectric module is now available through Thermal Electronics Corporation which could be used in the design of an exhaust system thermal generator. The module is a BiTe-PbTe hybrid (TEG1-PB-12611-6.0). The module features two optimized thermoelectric semi-conductors of N-type material and P-type material to form a hybrid thermoelectric generator module of improved performance and temperature stability. The modules are designed with high temperature bonding materials that allow them to withstand temperatures of up to 360°C. As long as the TEG thermoelectric power module is placed into a system, whereby the hot side is at a higher temperature than the cold side, DC power will be produced. The TEG1-PB class of module is able to operate continuously in higher temperatures than traditional thermoelectric power modules made from BiTe material only. The ceramic surfaces are covered with graphite sheets, which displaces the need for thermal grease. These novel TEG modules work best in the 200°C to 360°C temperature range and offer superior power output at temperatures above 260°C on the hot side, compared to standard BiTe modules. The P and N-type semi-conductors used in these new hybrid TEG modules offer the best performance and cost efficiencies of any module commercially available (Thermal Electronics Corporation).

Table 6 Performance specifications (Thermal Electronics Corporation)

Module TEG1-PB-12611-6.0			
Hot side temperature (℃)	350		
Cold side temperature (℃)	30		
Matched load resistance (Ω)	0.97		
Matched load voltage (V)	4.6		
Matched load current (A)	4.7		
Matched load power (W)	21.7		
Heat flow across module (W)	≈310		
Heat flow density ($W\ cm^{-2}$)	≈9.88		
Life expectancy	14 years @ 280℃	12 years @ 320℃	8 years @ 350℃

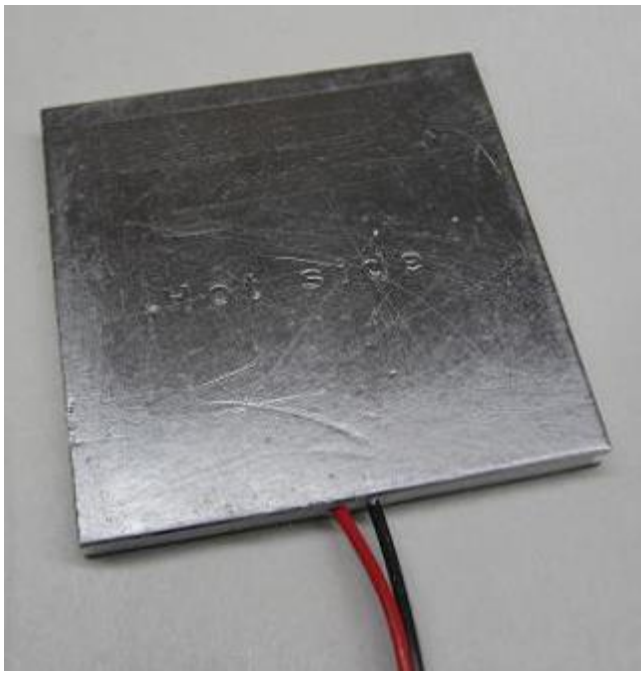

Figure 11 Hybrid TEG1-PB-12611-6.0 module (Thermal Electronics Corporation)

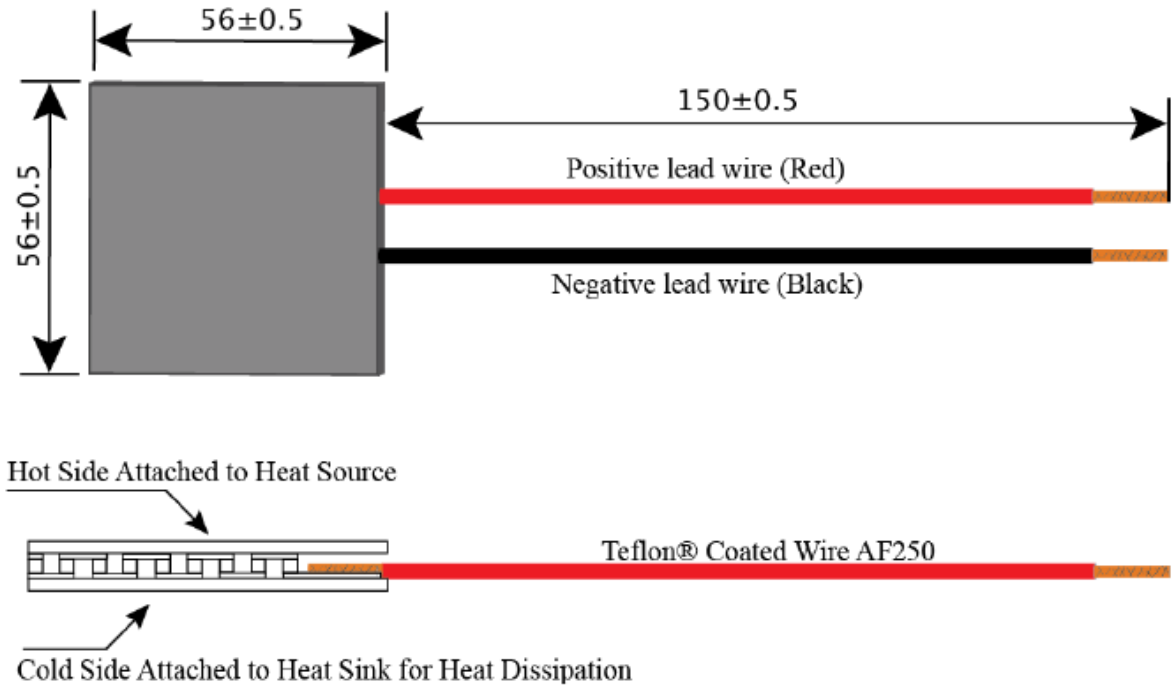

Figure 12 TEG1-PB-12611-6.0 module physical dimensions (Thermal Electronics Corporation)

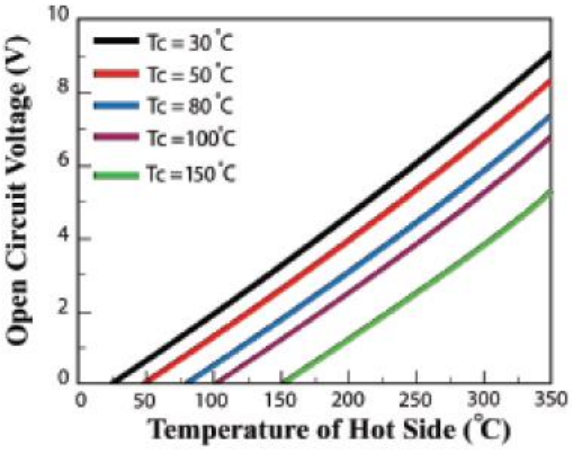

This chart shows open circuit voltage V_S T_h under various T_c .

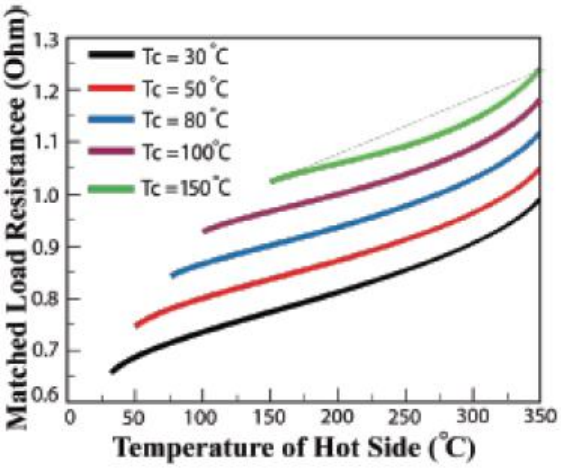

This graph shows open circuit voltage V_S T_h under various T_c .

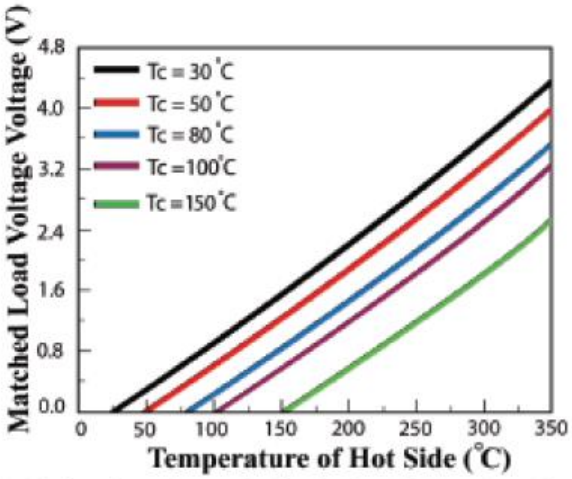

This chart shows the matched load voltage V_S T_h under various T_c.

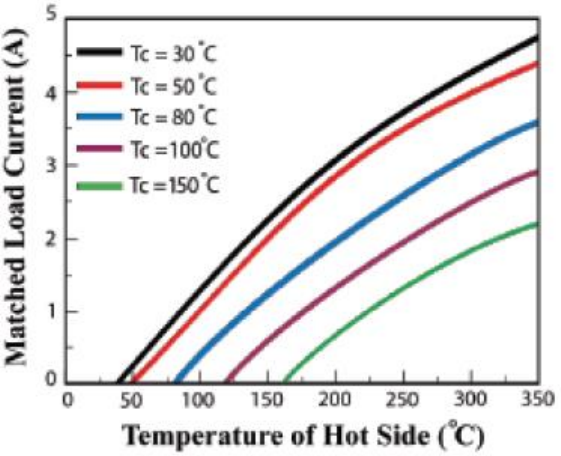

This chart shows the matched load voltage V_S T_h under various T_c .

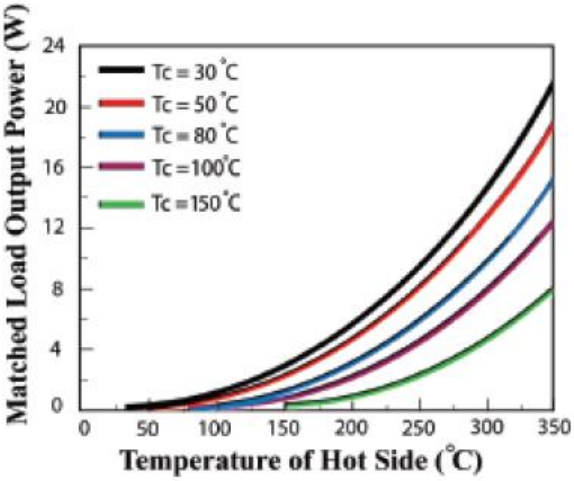

This chart shows the matched load output power V_S T_h under various T_c .

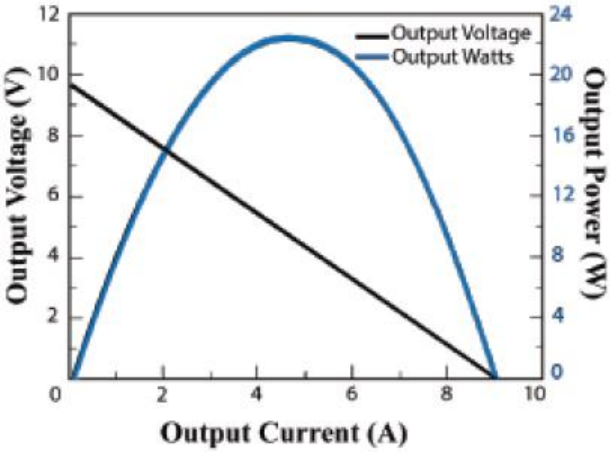

This chart shows output voltage and output power where V_S is output current under T_h = 300℃ and T_c = 30℃

Figure 13 TEG1-PB-12611-6.0 module performance parameters (Thermal Electronics Corporation)

4.2.2 Exhaust gas thermal generator configuration and performance

The thermal generators are mounted on the hot source of dimensions 112 × 112 × 504 mm. On each flat surface there would be 2 rows of 9 thermal generators. All thermal generators in the row are connected in series and then in parallel with all other rows.

Overall voltage of each row	$\boldsymbol{4.6 \times 9 = 41.4\ volts}$
Overall amperage of rows connected in parallel	$\boldsymbol{4.7 \times 8 = 37.6\ amps}$
Net power output	$\boldsymbol{41.4 \times 37.5 = 1552\ watts}$
Heat flow across each module	$\boldsymbol{310\ watts}$
Total heat flow on hot side	$\boldsymbol{310 \times 9 \times 8 = 22320\ watts}$

From equation 3.6b

$$\eta_t = \frac{W}{Q_h}$$

$$\eta_t = \frac{1552}{22320}$$

$$Thermal\ efficiency = 7\%$$

Total heat flow on cold side from equation 3.6c

$$Q_c = Q_h - W$$

$$Q_c = 22320 - 1552$$

$$Q_c = 20768\ watts$$

4.2.3 Hot source heat exchanger design

The hot side heat exchanger core consists of an Aluminum block of dimensions 112 × 112 × 504 mm. 25 holes of 10 mm diameter are drilled through the 504 mm length. Through these holes the engine exhaust gases will flow. Aluminum is the material recommended by Thermal Electronics Corporation for applications up to 400℃. The low weight and excellent thermal conductivity of Aluminum together with an acceptable melting point of 660℃ make Aluminum suitable material for this application.

The square shape of the heat exchanger core is necessary mainly because all available thermal generators are made flat and need to go on a flat surface. The main objective is to maximize the surface area contact with the thermal generators, and the square shape does that best, without having to resort to fins. The 25 holes of 10 mm diameter serve to maximize the area of contact between hot exhaust gases and the heat exchanger core.

The total area of the heat exchanger core in contact with thermal generators is 0.2258 m^2. The total area of the exhaust gases in contact with the heat exchanger core is 0.396 m^2.

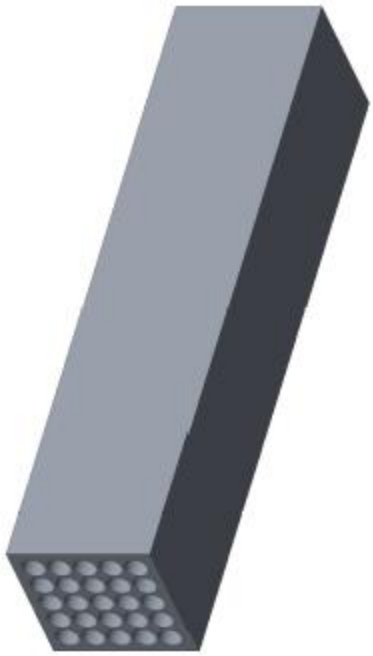

Figure 14 Heat exchanger aluminum core

Thermal generators in rows of 9 will be placed in pairs on each of the 4 heat exchanger core surfaces. All rows will be connected electrically in parallel with each other.

Figure 15 Thermal generator

4.2.4 Cold sink heat exchanger design

To maximize efficiency the cold side of the thermal generator will needs to be kept below a maximum temperature of 30℃. Excessive temperature of the cold side junction can also lead to failure of the thermal generator. Keeping the cold side to 30℃ or below is the optimal design and this can only really be achieve by liquid cooling. The liquid coolant will be circulated through 4 outer aluminum cooling ducts (Figure 16) by centrifugal electric pumps. The liquid will form part of a separate cooling system consisting of an air to liquid intercooler and cooling ducts as shown in Figure 16.

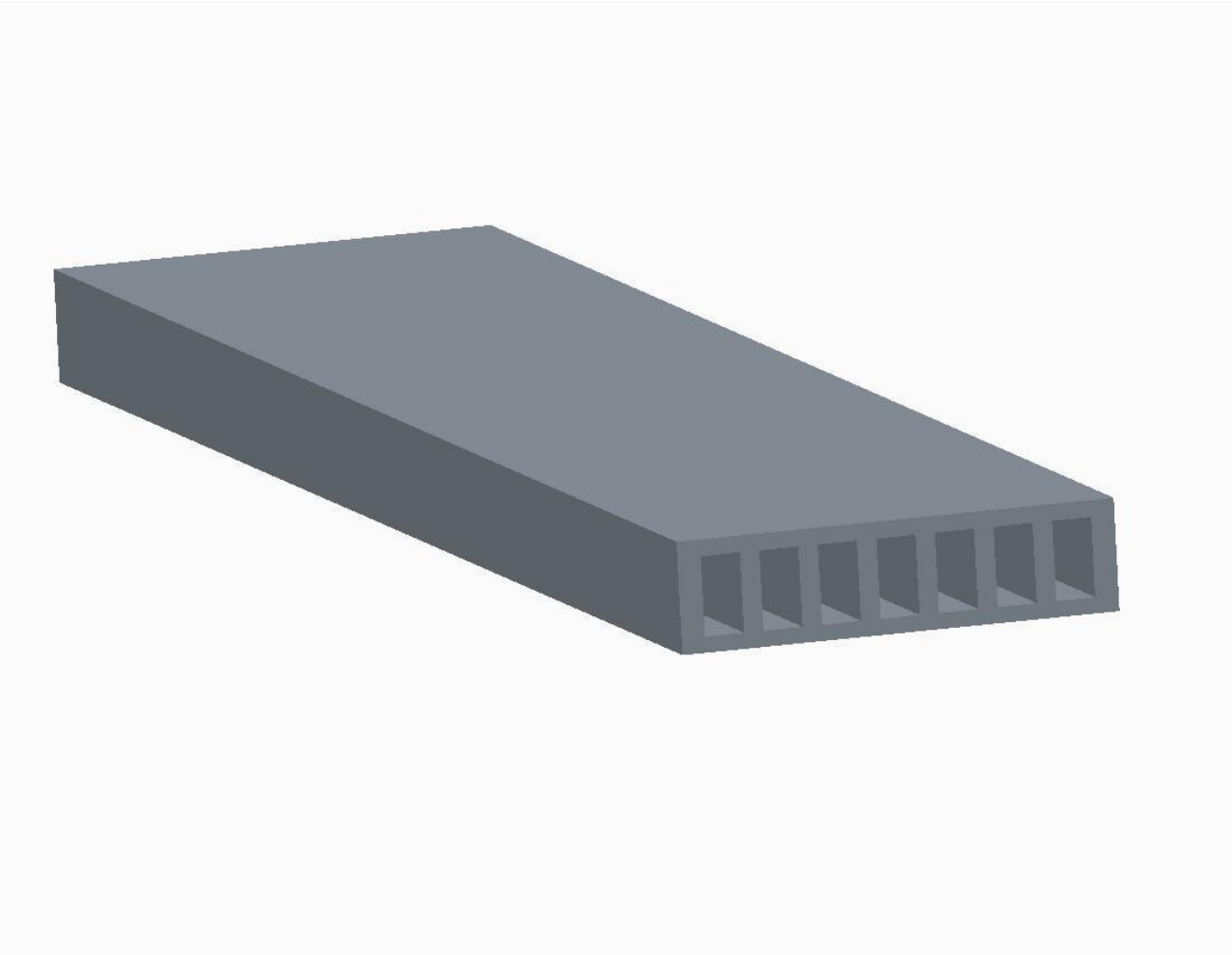

Figure 16 Aluminum cooling ducts

4.2.5 Thermal Generator design proposal

The proposed prototype thermal generator layout is shown in figure 17.

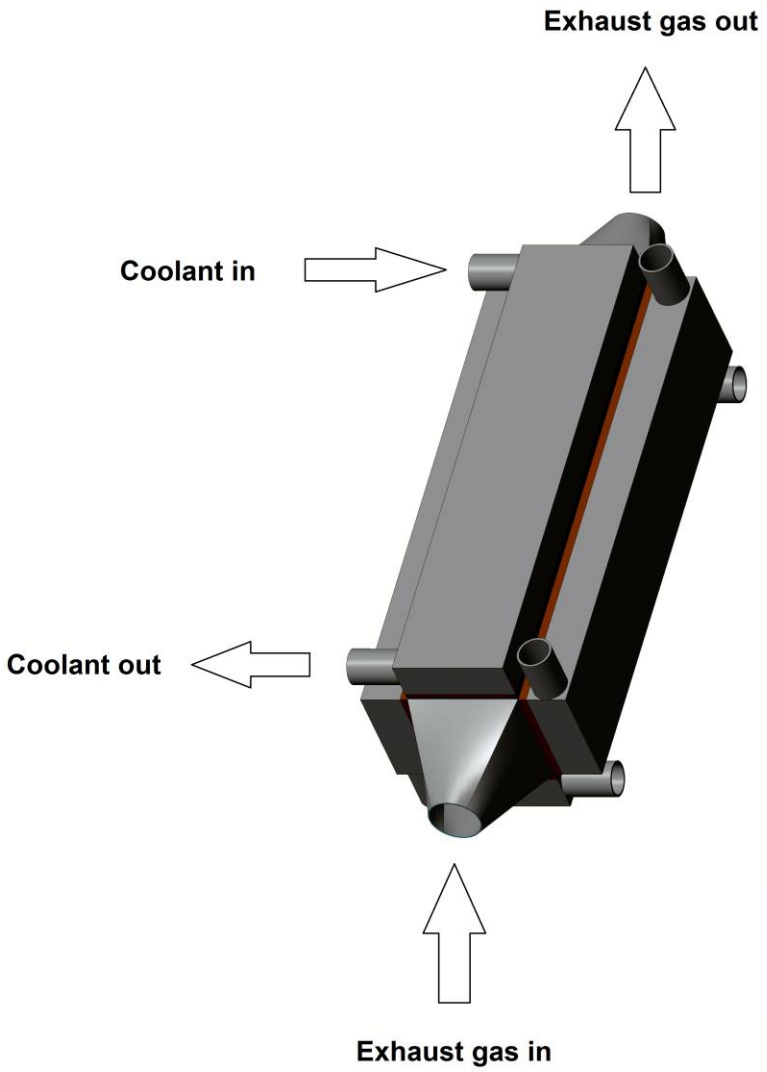

Figure 17 Assembled model of thermal generator

4.3 Thermal Analysis

A basic thermal analysis was conducted on the proposed TEG design using ANSYS 16.1 Academic Edition. The model was simplified with two plains of symmetry and substitution of the coolant cooling tubes and thermal electric generators by an equivalent convection cooling coefficient.

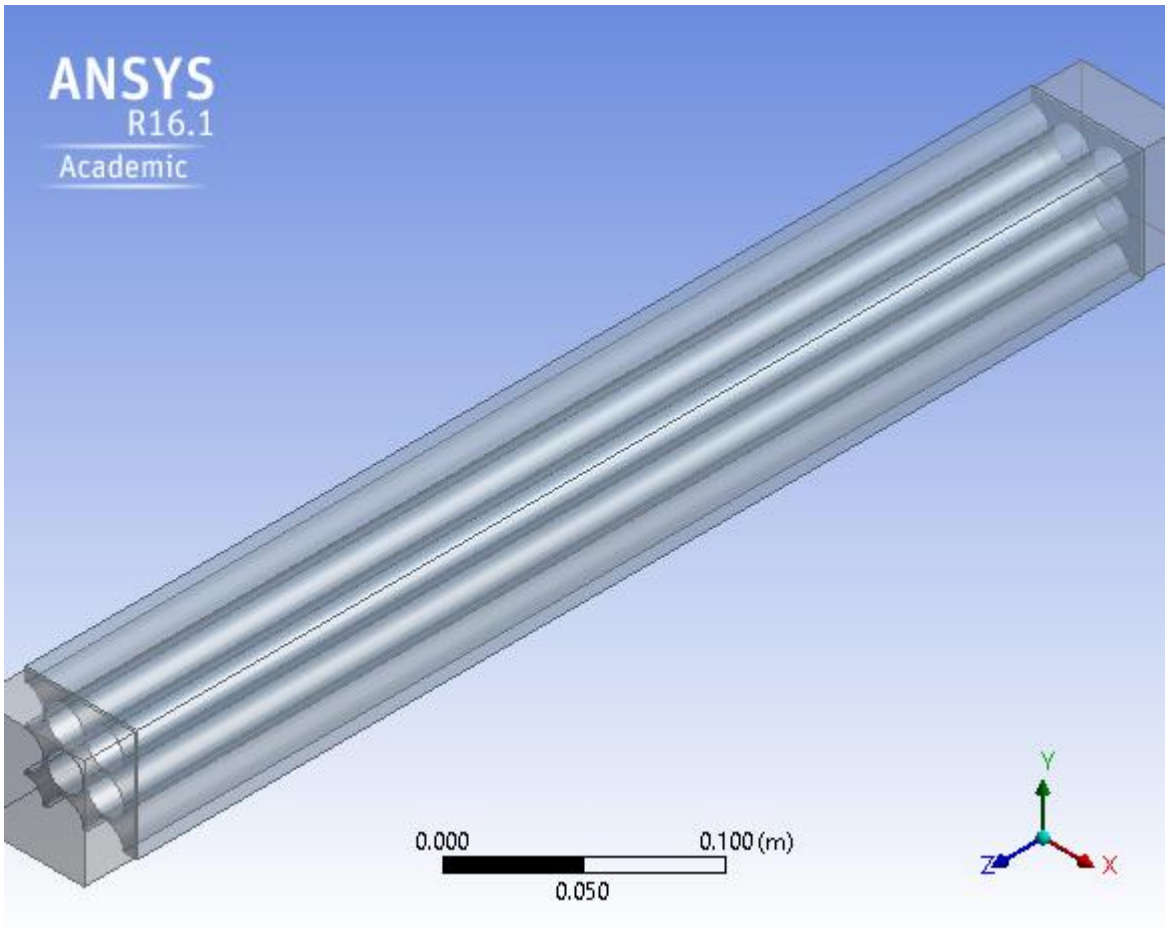

Figure 18 Fluid and Solid domains of model with 2 planes of symmetry.

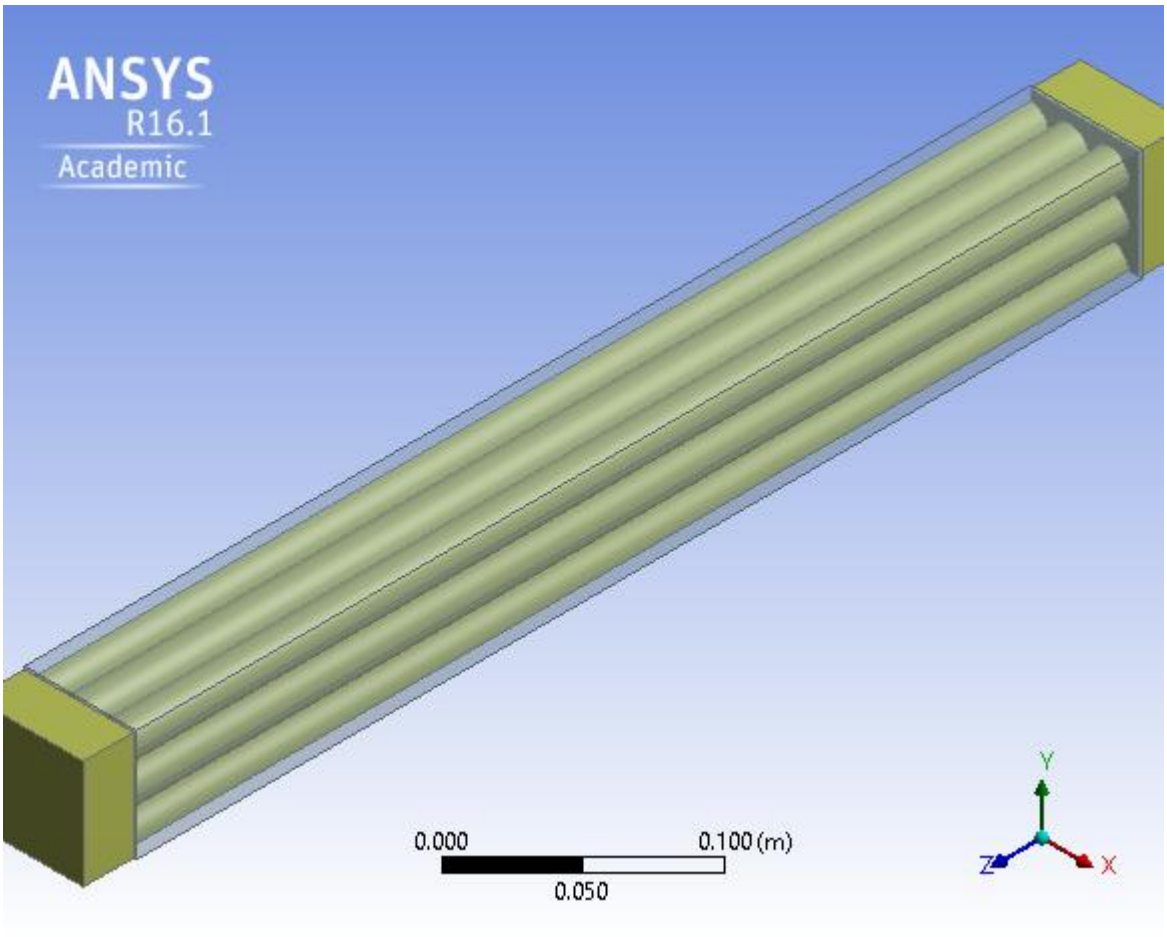

Figure 19 Fluid domain of model with 2 planes of symmetry

4.3.1 Simulation operating conditions

The exhaust gas mass flow rate, exhaust gas temperature and temperature difference between the hot and cold side of the thermal electric generator are key variables which are dependent on the engine size, configuration and operating conditions. Exhaust gas is a mixture of multiple gas compositions but consists predominantly of nitrogen. For the purpose of this simulation nitrogen gas is substituted for the exhaust gas in the simulated model. Exhaust gas is approximately 300-500 kpa in pressure and 500-700 ℃ in temperature when discharged from the exhaust port (Braess et al). After passing through the exhaust manifold and catalytic convertor the pressure approaches atmospheric and the temperature drops to 300-600℃. The initial temperature and flow rate of the exhaust gas at the inlet of the TEG is an important parameter as it determines how much heat energy is available for extraction. Typical operating condition are shown in Table 7.

Table 7 Typical engine operating conditions based on 1200cc engine

Driving cycle	Exhaust gas (g/s)	Exhaust gas temperature (K)
Urban	5.7	573.15
Suburban	14.4	673.15
Maximum power	80.1	873.15

4.3.2 Theory and boundary conditions

The computing domain consists of both solid and fluid portions. The temperature and flow fields of interest are obtained by solving a set of mathematical equations with respect to computational fluid and solid domains. In the fluid domain the equations of mass, momentum and energy conservation are solved to model fluid flow, heat and mass transfer. For the solid domain only the equation of heat transfer is solved.

Continuity equation:

$$\frac{\partial \rho}{\partial t} + \nabla . (\rho U) = 0$$

Momentum equation:

$$\frac{\partial (\rho U)}{\partial t} + \nabla (\rho U U) = -\nabla p + \nabla \tau + S_M$$

Energy equation:

$$\frac{\partial (\rho h_{tot})}{\partial t} - \frac{\partial p}{\partial t} + \nabla (\rho U h_{tot}) = \nabla (\lambda \nabla T) + \nabla (U \tau) + U S_M + S_E$$

The conservation of energy in the solid domain is:

$$\frac{\partial(\rho H)}{\partial t} + \nabla(\rho U_s h) = \nabla(\lambda \nabla T) + S_E$$

Where:

ρ = density

τ = stress tensor

λ = Thermal conductivity of solid

U = velocity

At exhaust gas pressure of atmospheric and temperatures of 600 ℃ the speed of sound is 515 m/s. This is much greater than the flow velocity. The flow field can therefore be considered as incompressible. The k-epsilon turbulence model was used to simulate the exhaust gas flow as it is the industrial standard for many commercial CFD models. Exhaust gas inlet velocity and temperature was set to the value of the respective driving cycles as shown in Table 7.

4.3.3 Model setup parameters

Table 8 Simulation model setup parameter

	Material	**Type**
Fluid	Nitrogen	N_2
Solid	Aluminum	T6061

	Velocity (m/s)	**Temperature (K)**	**Pressure (Gauge) pa**
Urban	4.87	573.15	0
Suburban	14.4	673.15	0
Maximum power	100.23	873.15	0

4.3.4 Results of thermal analysis

Urban cycle

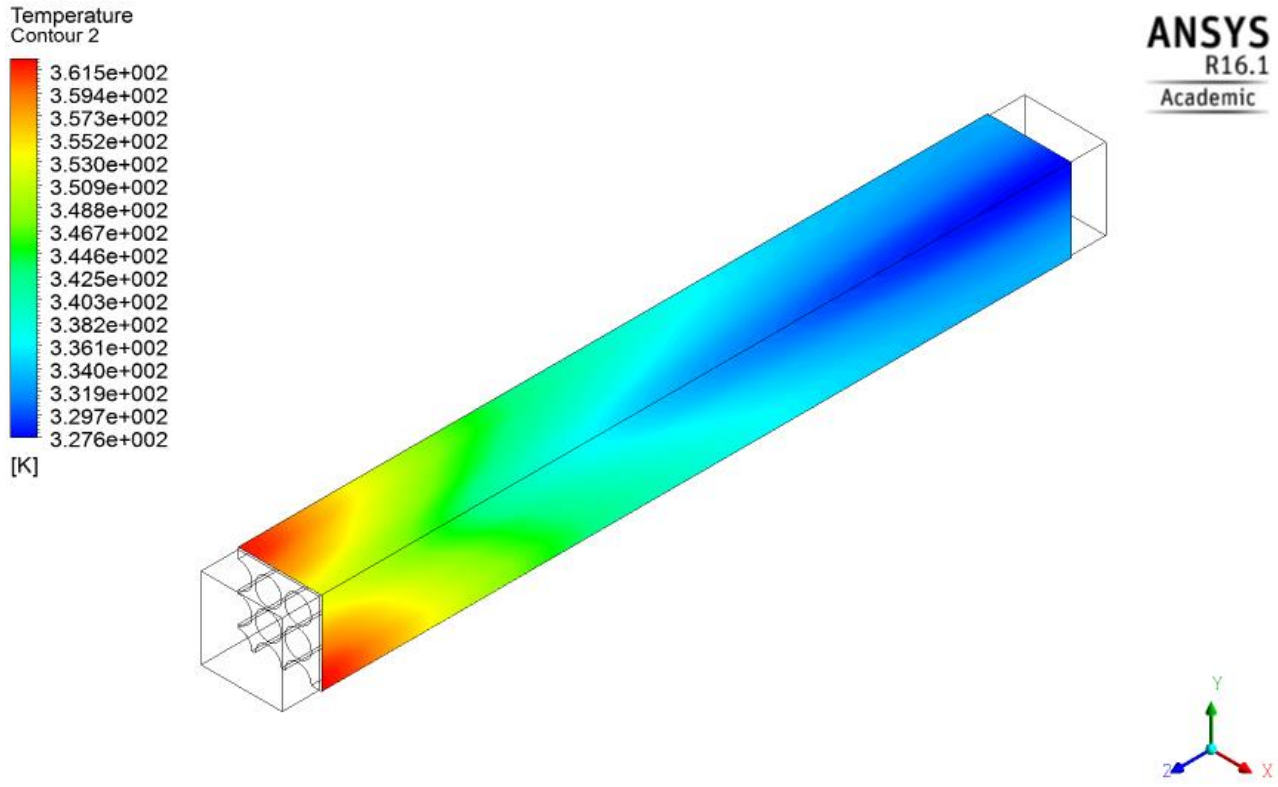

Figure 20 Temperature of hot side of TEG on urban cycle

Table 9 Output values on urban cycle

TEG hot side average temperature	339 K
Outlet gas temperature	467 K
Heat flow out of cooling surface	1302 w
Expected power output from TEG	91 w

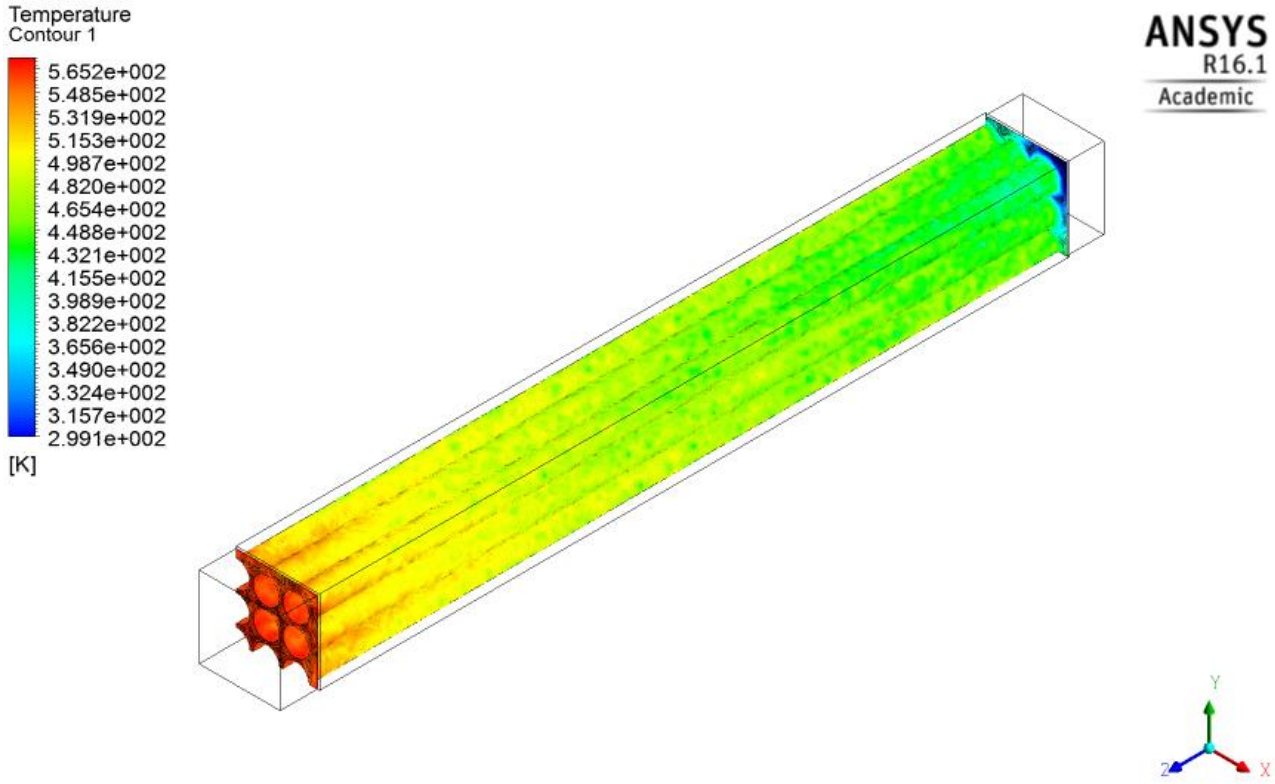

Figure 21 Internal fluid wall temperature on urban cycle

Suburban cycle

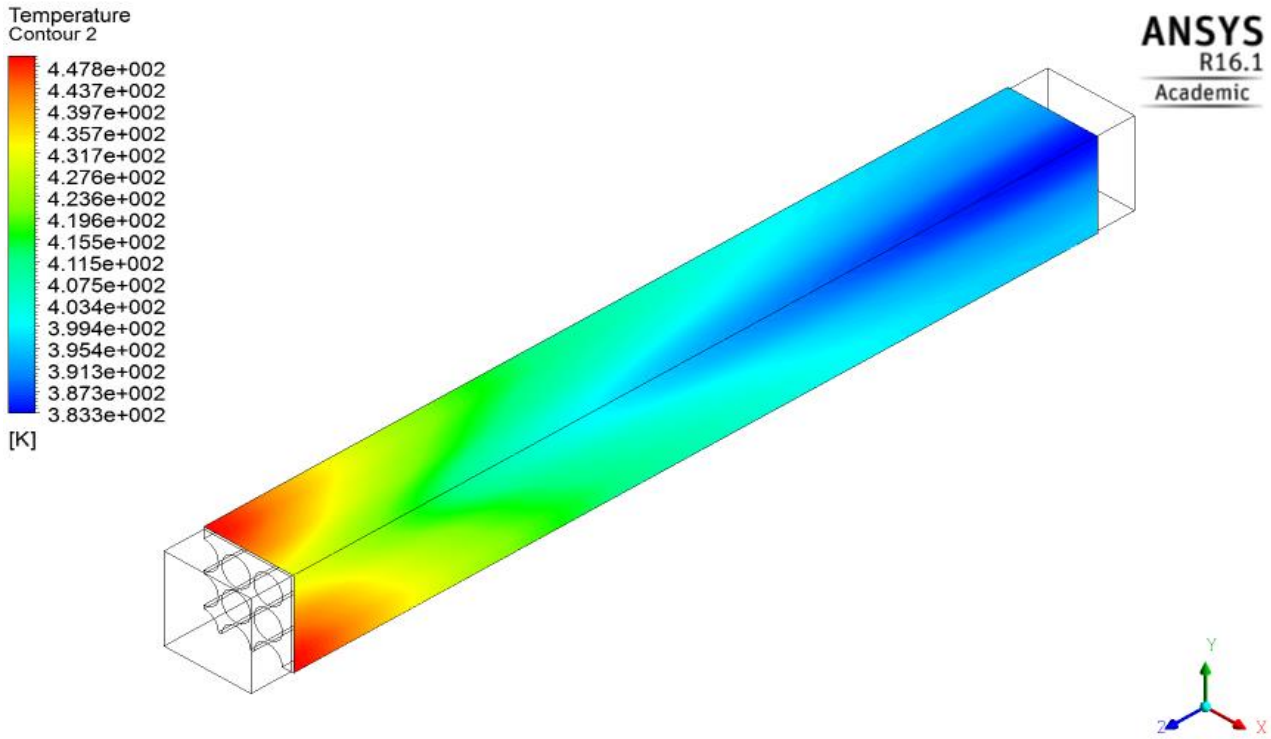

Figure 22 Temperature of hot side of TEG on suburban cycle

Table 10 Output values on suburban cycle

TEG hot side average temperature	407 K
Outlet gas temperature	543 K
Heat flow out of cooling surface	3210 w
Expected power output from TEG	225 w

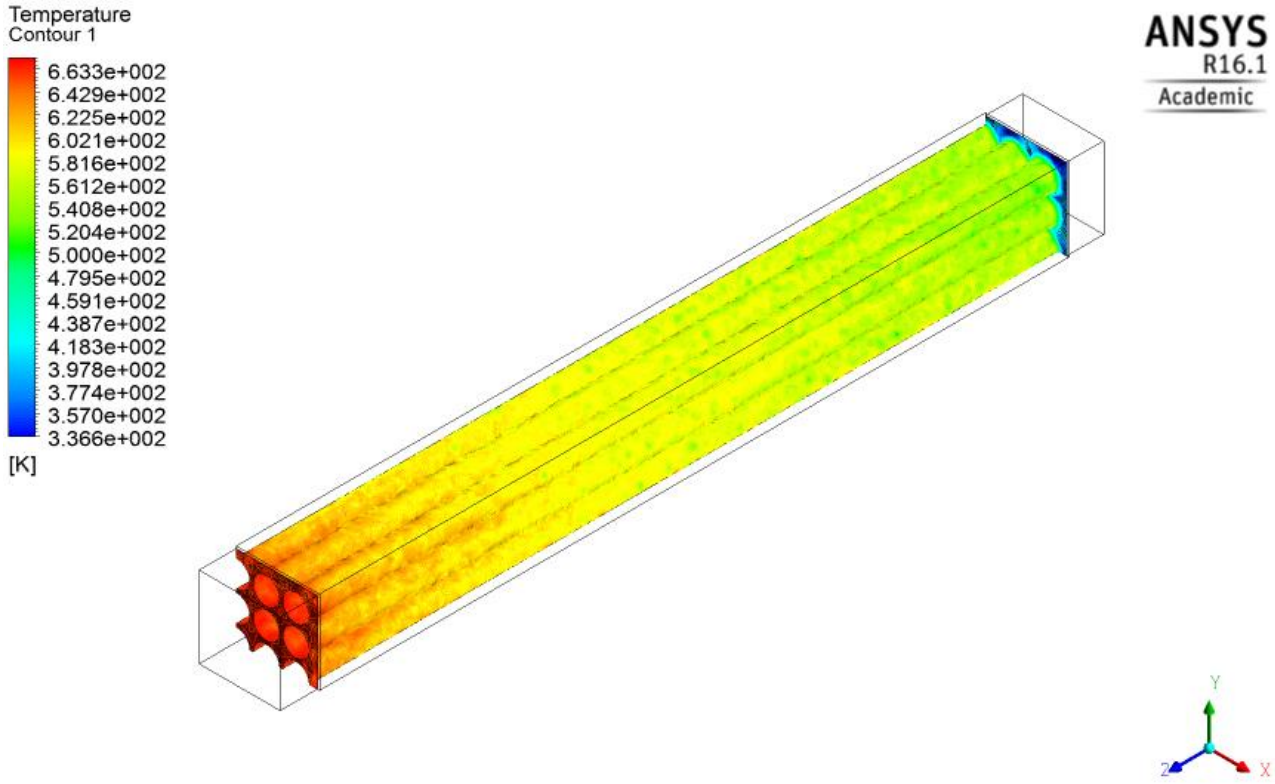

Figure 23 Internal fluid wall temperature on suburban cycle

Maximum power cycle

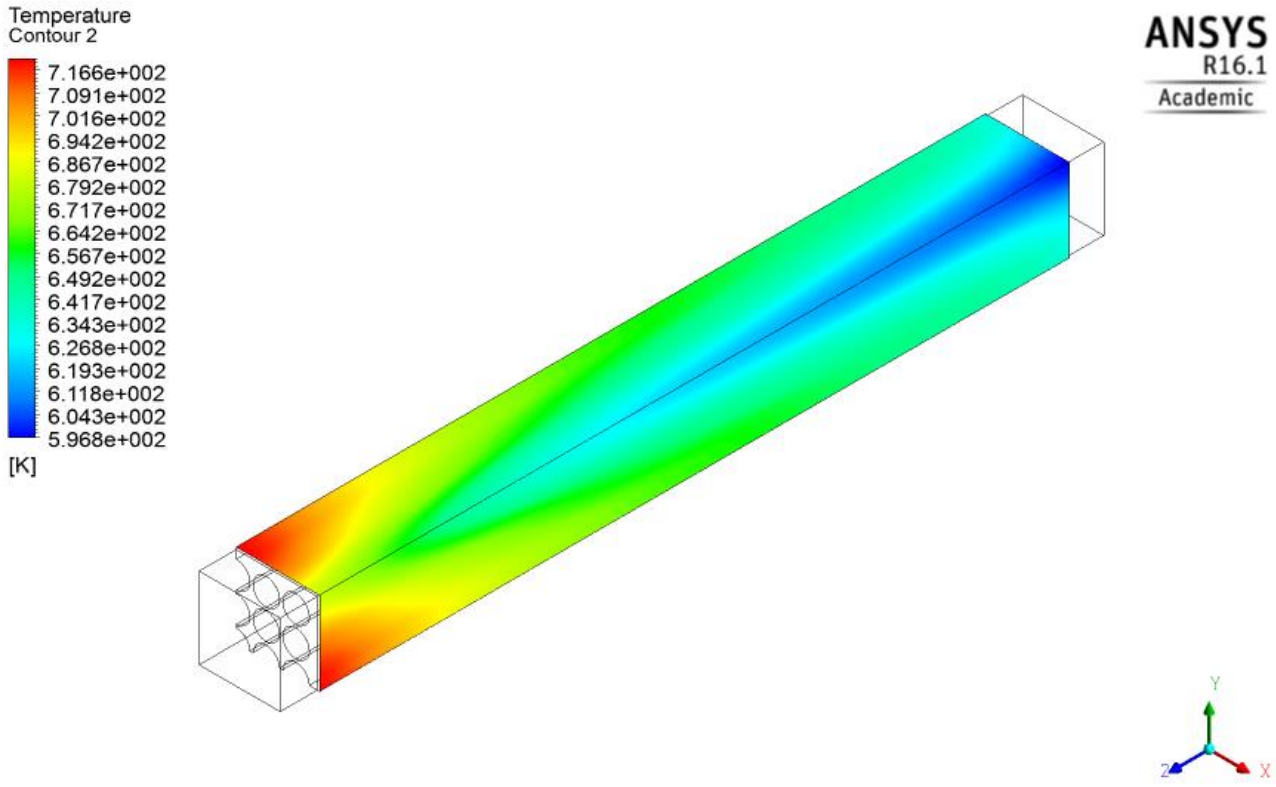

Figure 24 Temperature of hot side of TEG on maximum power cycle

Table 11 Output values on maximum power cycle

TEG hot side average temperature	651 K
Outlet gas temperature	739 K
Heat flow out of cooling surface	10107 w
Expected power output from TEG	708 w

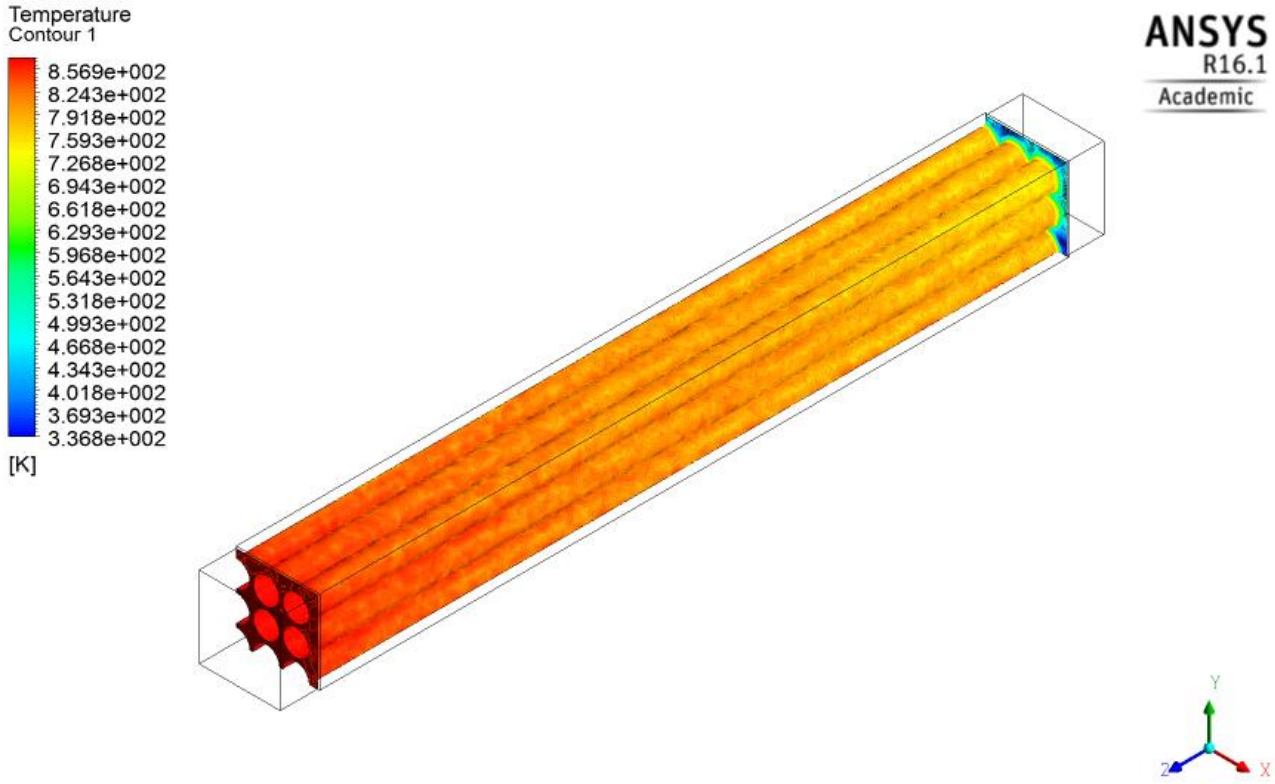

Figure 25 Internal fluid wall temperature on maximum power cycle

4.3.6 Results of analysis

The results show that the proposed design does not extract heat efficiently enough to reach the theoretical power limit of 1552 w. The heat flow out of the heater core in the suburban cycle is given in the simulation as 3210 w of which an estimated 7% could be converted to electrical power giving an output of 225 w.

It is noted that the exhaust gas outlet temperature is 543K. This indicates that a significant amount out thermal energy has not been recovered from the exhaust gas. The design of the thermal generator may need to be improved to increase the efficiency. Possible design improvements could be to increase the length of the design, or reduce the size and increase the number of the tubes. Both these suggestions would increase the surface area of contact between the exhaust gas and the heater core. A third alternative could be to use a second thermal generator in series with the first.

Increasing the length of the thermal generator from 504 mm upwards could potentially lead to fitment or location issues. If the length were doubled, this would mean that a suitable location under the vehicle of 1008mm straight length would need to be found. It would be more sensible and just as effective to use the 504mm design coupled with an insulated, and shaped to suit, junction pipe.

Tables 13 to 15 show the results of a simulation of 6 thermal generator in series.

Table 12 Urban driving simulation results

Urban driving	Outlet Temperature (K)	Heat flow out (w)	Output power (w)
TEG 1	467	1302	91
TEG 2	401	805	56
TEG 3	360	498	34.9
TEG 4	335	309	21.6
TEG 5	320	193.5	13.6
TEG 6	311	124.4	8.7
		Total	**226**

Table 13 Suburban driving simulation results

Suburban driving	Outlet Temperature (K)	Heat flow out (w)	Output power (w)
TEG 1	543	3210	225
TEG 2	463	2102	147.2
TEG 3	409	1425	99.8
TEG 4	372	971	68
TEG 5	347	660.5	46.3
TEG 6	331	451.3	31.6
		Total	**618**

Table 14 Maximum power simulation results

Maximum power	Outlet Temperature (K)	Heat flow out (w)	Output power (w)
TEG 1	738.9	10107	707.5
TEG 2	635.2	7725.5	540.8
TEG 3	555.5	5907.5	413.5
TEG 4	494.5	4521	316.5
TEG 5	447.9	3465.5	242.6
TEG 6	412.4	2661.8	186.3
		Total	**2407**

To increase the efficiency of each individual TEG it may be possible to reduce the hole size and count from 25 at 10 mm to 225 at 3 mm. The table below shows the comparative flow direction areas and exhaust gas to solid core contact area.

Table 15 Heater core hole / area comparison

	Fluid/Solid surface interface (m^2)	**flow direction area** (m^2)
25 holes at 10 mm	0.396	0.001963
225 holes at 3 mm	1.069	0.00159

Reducing hole size and increasing the hole count from 10 at 25 to 3 at 225 increases the exhaust gas contact area by a factor of 2.7 and marginally reduces the flow area by a factor of 1.2. Reducing flow area also increases the velocity of flow in the tubes thereby increasing the heat transfer coefficient between the exhaust gases and the heater core.

4.3.6 Analytical analysis

The performance of the thermal generator was analyzed by estimating the thermal resistance of each component/junction in the unit. The overall thermal resistance was calculated from the components and the power flow through the generator was then calculated. The critical components/junction are:

- Exhaust gas to core interface heat transfer coefficient
- Aluminum core conduction
- TEG conduction
- TEG to coolant interface heat transfer coefficient

Assumptions

- Thermal resistance of interface between Aluminum core and TEG in negligible
- Thermal resistance of interface between TEG and Coolant housing negligible.
- Thermal resistance of coolant housing negligible.
- Exhaust gas flow in heater core is turbulent at all time.
- Heat transfer coefficient ($\overline{h_c}$) for cold coolant side is a constant $500\ w/m^2k$.
- Temperature of coolant in is $\approx$ temperature of coolant out.

Considering Urban cycle (Table 7) with exhaust gas flow of 5.7g/s at 573.15K

$$\boldsymbol{V_{Urban} = \frac{\dot{m}}{\rho A}}$$

$$V_{urban} = \frac{5.7}{596 \times 0.25\pi \times 0.01^2 \times 25}$$

$$V_{Urban} = 4.87 m/s$$

Similarly

$$V_{Suburban} = 14.44 m/s$$

$$V_{Max\ power} = 100.23 m/s$$

Calculating Reynolds number for each flow rate:

$$Re = \frac{\rho V D}{\mu}$$

$$Re_{Urban} = \frac{0.596 \times 4.87 \times 0.01}{29.322 \times 10^{-6}}$$

$$Re_{Urban} = 989.88$$

Similarly

$$Re_{Suburban} = 2239.58$$

$$Re_{Max\ power} = 10630.26$$

Due to pulsating flow of exhaust gasses and sharp entry into thermal generator it is assumed that the exhaust gas flow is turbulent through the whole generator length. Reynolds number is therefore increased by a factor of 2.5

Table 16 Flow velocity and Reynolds numbers of driving cycles

Driving cycle	Exhaust gas (g/s)	Exhaust gas temperature (K)	Velocity (m/s)	Reynolds number
Urban	5.7	573.15	4.87	2475
Suburban	14.4	673.15	14.44	5599
Maximum power	80.1	873.15	100.23	26576

Using Dittus-Boelter equation for exhaust gas to heater core interface

$$\overline{Nu_D} = \frac{\overline{h}_c D}{k} = 0.023 Re^{0.8} Pr^{0.3}$$

$$\overline{h_{c_{Urban}}} = \frac{k}{D} 0.023 Re^{0.8} Pr^{0.3}$$

$$\overline{h_{c_{Urban}}} = \frac{0.0429}{0.01} 0.023 \times 2475^{0.8} \times 0.71^{0.3}$$

$$\overline{h_{c_{Urban}}} = 46.2\ w/m^2K$$

Similarly

$$\overline{h_{c_{Suburban}}} = 100.7\ w/m^2K$$

$$\overline{h_{c_{Max\ power}}} = \ 420.5\ w/m^2K$$

The heat power flow through the thermal generator is given by the equation:

$$Q = \frac{\Delta T}{R_{Ex} + R_{Core} + R_{TEG} + R_{Coolant}}$$

Where

For Urban cycle

$$R_{Ex} = \frac{1}{\overline{h_c} A} = \frac{1}{46.2 \times \pi \times 0.01 \times 25 \times 0.504} = 0.055\ K/m$$

Suburban cycle

$$R_{Ex} = \frac{1}{\overline{h_c} A} = \frac{1}{100.7 \times \pi \times 0.01 \times 25 \times 0.504} = 0.025\ K/m$$

Max power

$$R_{Ex} = \frac{1}{\overline{h_c} A} = \frac{1}{420.5 \times \pi \times 0.01 \times 25 \times 0.504} = 0.006\ K/m$$

$$R_{Core} = \frac{L}{kA} = \frac{0.0382}{250 \times \pi \times 0.05 \times 0.504} = 0.00193\ K/m$$

$$R_{TEG} = \frac{L}{kA} = \frac{0.003}{1.2 \times 0.112 \times 0.504 \times 4} = 0.0111\ K/m$$

$$R_{Coolant} = \frac{1}{\overline{h_c} A} = \frac{1}{500 \times 0.112 \times 0.504 \times 4} = 0.00886\ K/m$$

Estimation of heat power flowing through TEG in urban cycle.

$$\boldsymbol{Q_{TEG} = \frac{\Delta T}{R_{Ex} + R_{Core} + R_{TEG} + R_{Coolant}}}$$

$$\boldsymbol{Q_{TEG} = \frac{(573.15 - 293)}{0.055 + 0.00193 + 0.0111 + 0.00886}}$$

$$\boldsymbol{Q_{TEG} = 3643\, w}$$

Estimation of heat power flowing through TEG in Suburban cycle.

$$\boldsymbol{Q_{TEG} = \frac{(573.15 - 293)}{0.025 + 0.00193 + 0.0111 + 0.00886}}$$

$$\boldsymbol{Q_{TEG} = 5975\, w}$$

Estimation of heat power flowing through TEG in Max power cycle.

$$\boldsymbol{Q_{TEG} = \frac{(573.15 - 293)}{0.006 + 0.00193 + 0.0111 + 0.00886}}$$

$$\boldsymbol{Q_{TEG} = 10039\, w}$$

4.3.7 Comparison between CFD and analytical analysis

Table 17 Output comparison between analytical analysis and CFD

Exhaust gas flow rate (g/s)	Power output Analytical	Power output CFD
5.7	255	91
14.4	418	225
80.1	702	707

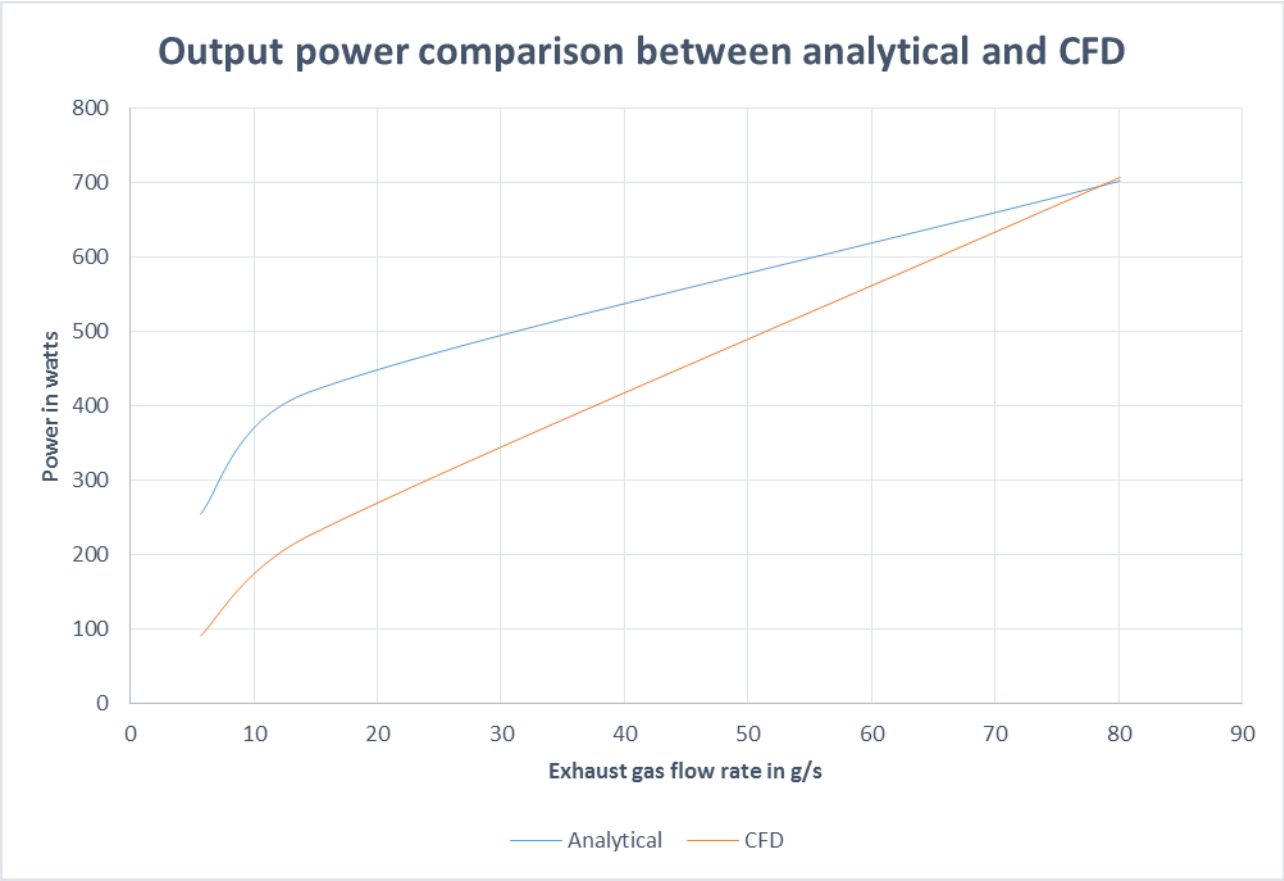

Figure 26 Output comparison between analytical analysis and simulation

4.3.8 Analysis conclusion

The simulation results showed the power producing capabilities of the TEG are limited by the speed of the exhaust gas flow and the surface area that can be achieved in one TEG. The problem can be alleviated by using a number of TEG units in series or increasing the exhaust gas surface contact within one unit. The thermal electric generator design presented is clearly not an optimum design for maximum power output.

The criteria for optimum thermal electric generator output is:

1) Maximize exhaust gas speed across heater core.
2) Maximize surface area of contact between exhaust gas and heater core.
3) Maintaining cold side temperature as low as possible

The simulation with 6 TEG units in series produced a constant 226 w under the urban driving profile, 618 w under the suburban driving profile and 2407 w under maximum load.

Chapter 5

Application

5.1 Introduction

Other than the battery and starter motor loads, the loads placed on a vehicle charging system can be considered to be either continuous loads, prolonged loads or intermittent loads. The charging system needs to be able to cope with these loads under all operating conditions. To have an estimation of the required output by the vehicle charging system, the power used by each individual component is measured and then added together. This includes the power required to charge the battery. The typical electrical power requirements of various vehicle systems are listed in Table 18.

Table 18 Estimated electrical power requirements for a typical vehicle

Continuous load	**Power (W)**	**Current (A) at 14V**
Ignition	30	2
Fuel Injection	70	5
Fuel pump	70	5
Instruments	10	1
Prolonged Loads	**Power (W)**	**Current (A) at 14V**
Park lights	30	2
Number plate lights	10	1
Headlight main beams	200	15
Headlight dip beams	160	12
Dash lights	25	2
Radio	15	1
Intermittent Loads	**Power (W)**	**Current (A) at 14V**
Heater	50	3.5
Indicators	50	3.5
Brake lights	40	3.0
Front wipers	80	6.0
Rear wipers	50	3.5
Electric windows	150	11.0
Radiator cooling fan	150	11.0
Heater blower motor	80	6.0
Heated rear window	120	9.0
Interior lights	10	1.0
Horns	40	3.0
Rear lights	40	3.0
Reversing lights	40	3.0

Auxiliary fog/spot lamps	110	8.0
Cigarette lighter	100	7.0
Headlight wash wipe	100	7.0
Seat movement	150	11.0
Seat heater	200	14.0
Sun-roof motor	150	11.0
Electric mirrors	10	1.0
Total	**1700 Watts**	**126 A**
Continuous load	180	13
Prolonged Loads	440	33
Intermittent Loads $\times$ 0.1	172	13
Total	**800 Watts**	**65 A**

Intermittent loads are used infrequently and are often coupled with a timer relay of some sort in order to prevent over use of that circuit. Assuming normal operating conditions a factor of 0.1 can be applied to the intermittent load total (Table 18). This gives an estimate for a typical alternator charging system requirement of 800 Watts for a modern day vehicle. However some luxury vehicle available in 2015 do have alternators rated at 1800 Watts.

The demand on the vehicle electrical system is constantly increasing. New technologies such as electrically pre-heated catalytic converters, electrically assisted power steering and heated windscreens are expected to see the demands on the vehicle electrical system continue to grow. Some typical electrical loads expected in the near future are shown in Table 19. As can be seen most are continuous and therefore will substantially increase the demand on the vehicle electrical system.

Table 19 Expected future electrical systems (Rashid 2011)

Exhaust air pump	300	Continuous
Electrohydraulic power steering	1000	Prolonged
Electric engine fan	800	Continuous
Heated catalytic convertor	3000	Continuous
Heated windshield	2500	Intermittent
Electromechanical engine valves	2400	Continuous
Active suspension	12000	Continuous

5.1.1 Estimation of electrical system loading

Table 20 shows the common electrical loads operating on a conventional motor vehicle and a corresponding estimated hourly usage in a 24 hour cycle. 3 estimations are presented, namely average loading, heavy loading and extreme loading. The input from a TEG based on suburban cycle driving is also shown in Table 20.

Table 20 Common electrical loads and corresponding estimated use in 24 hour cycle

Electrical system	Power (Watts)	Average (hours)	Heavy (hours)	Extreme (Hours)
Headlights	-200	12	19	24
Number plate	-10	12	19	24
Park lights	-30	12	19	24
Dash lights	-25	12	19	24
Radio	-15	4	8	24
Interior fan	-80	4	12	24
Engine management	-180	24	24	24
Wind screen wipers	-80	1	5	16
Electrical power steering	-1000	1	1	1
Indicators	-50	1	2	5
TEG input	618	24	24	24

The estimation of loading is very subjective and as such could vary extensively from vehicle make and model, driver habits and style as well as operating and climatic conditions.

As can be seen from Figure 27 and 28, under average and heavy driving conditions the proposed thermal generator can match the demands of the vehicle electrical system, even at light engine loads such as the suburban cycle driving pattern. Under extreme driving conditions (Figure 29) and suburban cycle load the thermal generator does not keep up with the demand and majority of the time in the 24 hour cycle the demand exceeds the thermal generator output. The estimated extreme driving condition is certainly extreme with most of the major electrical loads used constantly in a 24 hour cycle. While this extreme loading would certainly be unusual, there is still a possibility that it may occur.

The results of this simple model shows that an exhaust gas thermal generator can match and exceed the electrical system demand for the vast majority time. However in the interests of vehicle safety and reliability an alternator or back up charging system will most likely still need to be fitted for unusual situation where the thermal generator cannot keep up with the demand.

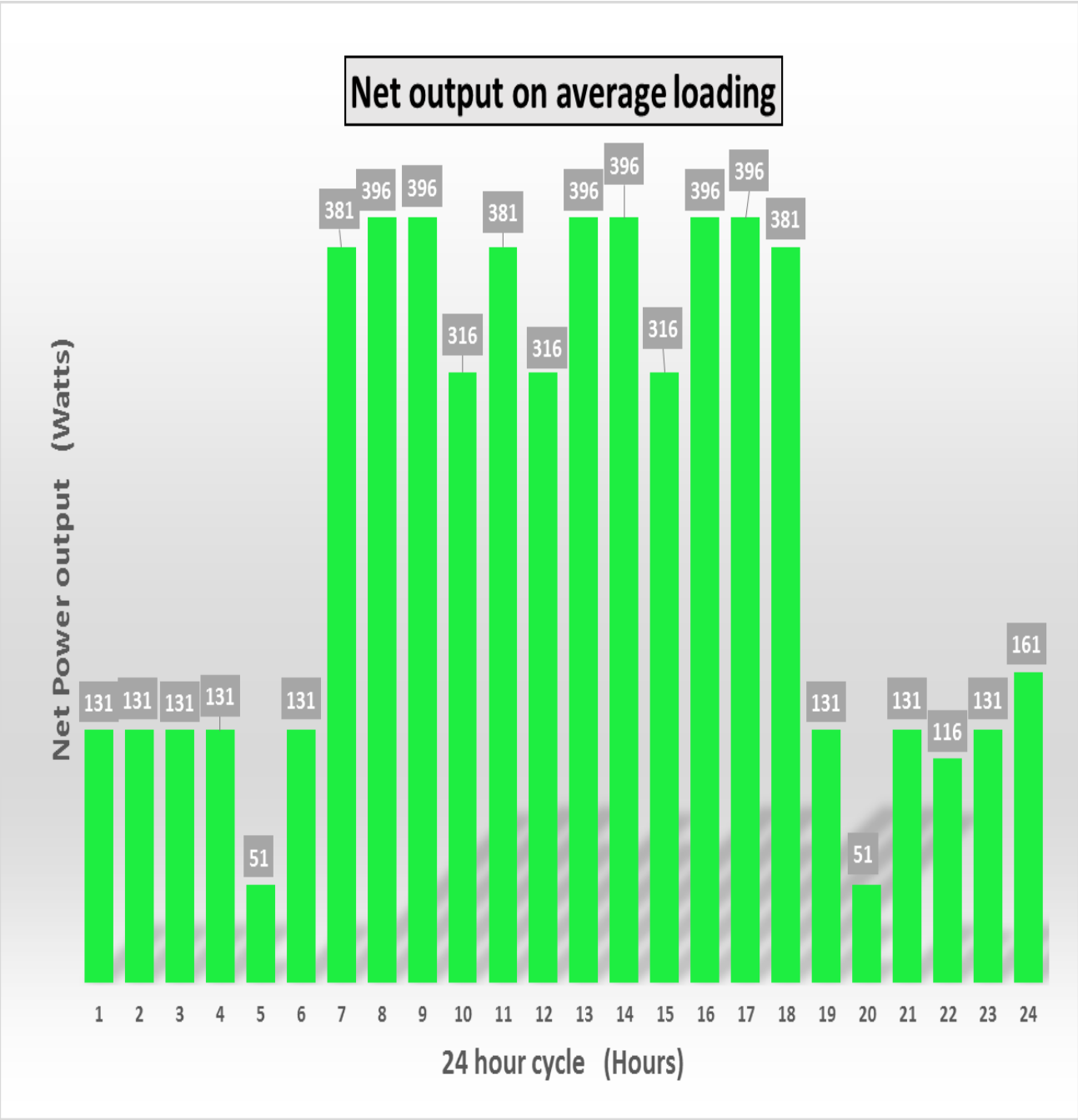

Figure 27 Net power output for Average electrical loading with driving on suburban cycle.

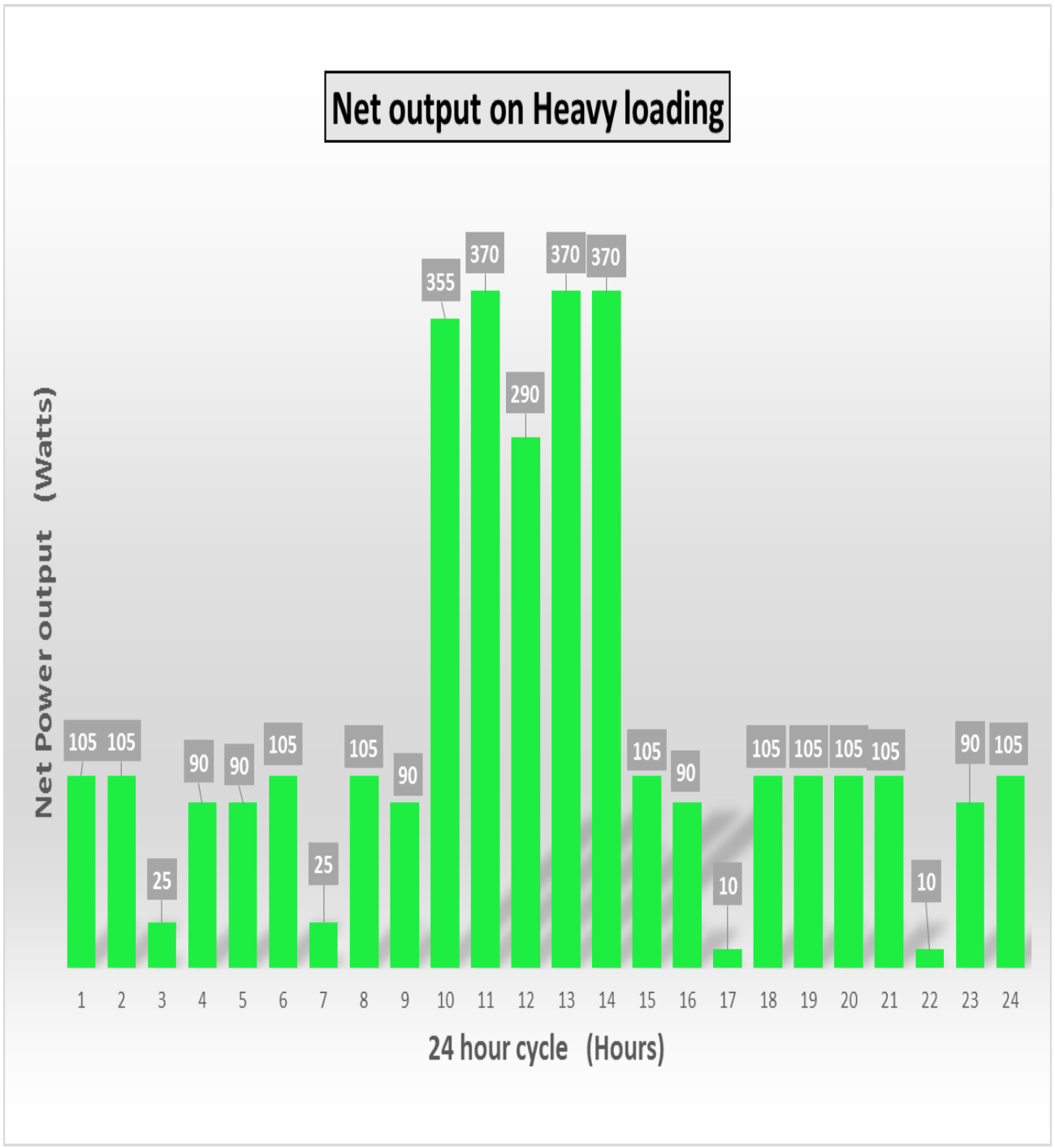

Figure 28 Net power output for Heavy electrical loading with driving on suburban cycle.

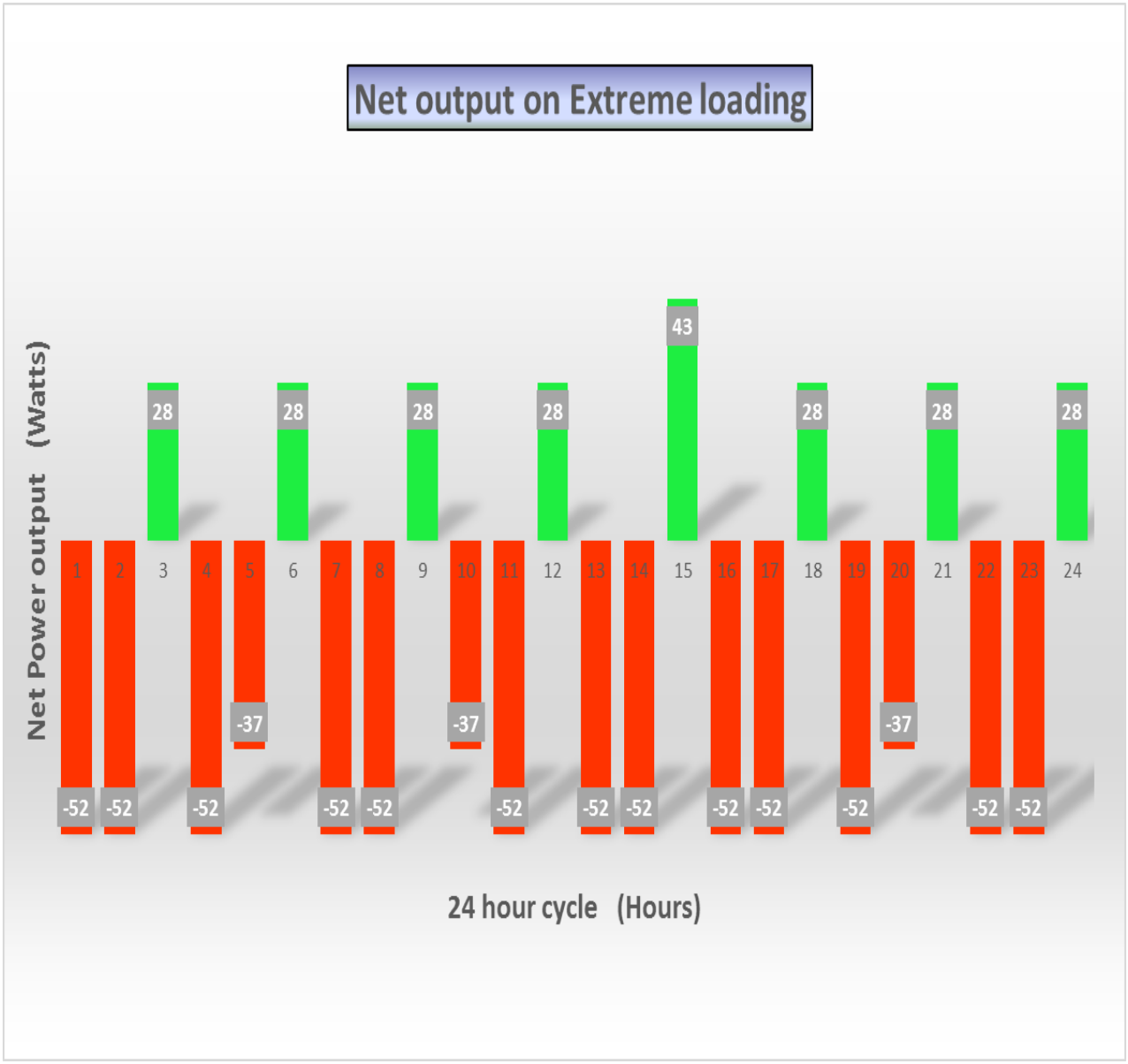

Figure 29 Net power output for Extreme electrical loading with driving on suburban cycle.

Table 21 Net power output for electrical loading on suburban cycle

Electrical loading	Net output (w)
Average	246
Heavy	139
Extreme	-23

5.2 Battery charging system

A thermal Electric Generator as proposed in the design should have enough electrical power to adequately power an average 12 volt automotive electrical system under normal operating conditions. The voltage and current should exceed the average requirements of the vehicle electrical system. In a conventional alternator vehicle charging system if the battery is fully charged the alternator charge rate can be reduced by a voltage regulator which controls the DC current flow through the rotor. In other words the alternator can simply be turned off to prevent over charging of the battery. Alternator output can be increased to match electrical system demand. A TEG output does not have the same quality of output control. As long as there is a temperature difference across the thermal module then electric power will be generated. A charge control unit would be required to regulate battery voltage to around 13.8 Volts and sense the battery level of charge. When battery is fully charged the electrical power would need to be dissipated over another load. It makes sense for this load would be something useful.

Even when not charging the Alternator components are still turning causing an inertial and friction load on the engine. In the case of a thermal generator there is no inertial, friction or charging load on the engine.

5.3 Hydrogen generator

5.3.1 Benefits of hydrogen addition

A potential use of the excess electrical energy could be to power a hydrogen producing cell. There are many hydrogen producing cell kits commercially available. These kits are powered directly by the vehicle battery and the hydrogen and oxygen mixture that is produced is returned to the engine via the inlet manifold. Suppliers of conventional systems running off alternator charged batteries claim very promising improvements in fuel economy. However these claims are not without much public debate.

First impressions of this system by somebody that is training in an engineering or technical background is that this cannot really be the case. The hydrogen is produced indirectly by the engine power. It would appear that this system is in conflict with the first law and second law of thermodynamics which states that energy cannot be created or destroyed and when transformed from one form to another there is always a loss. How is it possible to transform mechanical energy to hydrogen and then combust the hydrogen created and end up with more power? It certainly does not seem intuitively correct. The answer lies in how the introduced hydrogen combusts with the initial hydrocarbon fuel.

Suzuki and Sakurai (2006) conducted research into the effects of a hydrogen gas and petrol fuel co-combustion on a spark ignition internal combustion engine. The results showed up to a 40% increase in thermal efficiency under low load conditions compared to petrol combustion only. Additionally there was virtually no NO_x produced under light load conditions. A normal petrol engine

produces most of its NO_x products during these light load lean burn conditions. As engine load increased in the mixed fuel system the NO_x production increased drastically and the improvement in thermal efficiency diminished. The results showed very substantial improvements in thermal efficiency and reduction in NO_x emissions during light load conditions. A similar report by Cassidy JF (1997) verified the results by Suzuki and Sakurai as far back as 1977. Cassidy conducted a comparison between regular petrol, a bottled hydrogen-petrol mix and a hydrogen-petrol mix where the hydrogen was generated on the vehicle by a commonly used methanol reformer system. The effect of hydrogen increasing the apparent flame speed at low equivalence ratios was verified.

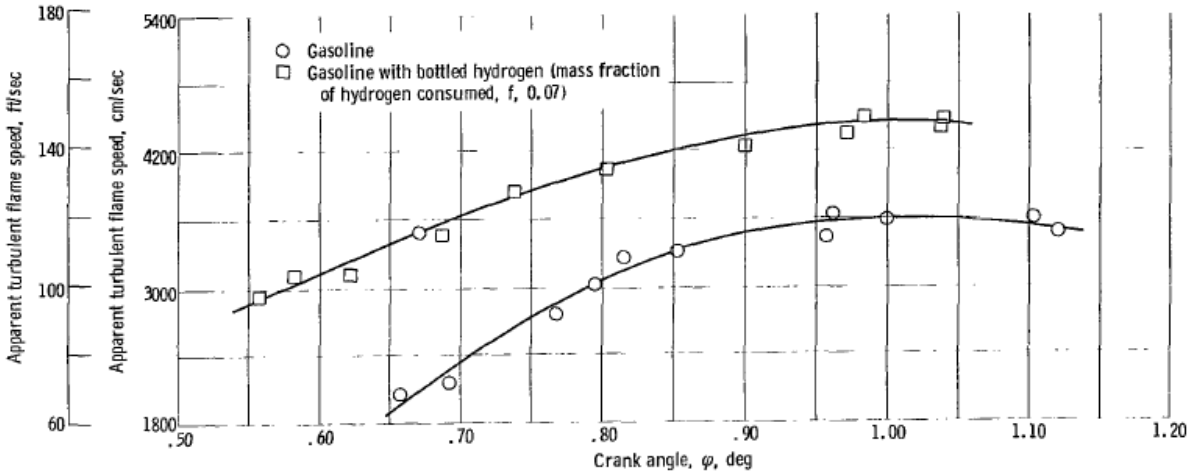

Figure 30 Apparent turbulent flame speed as a function of equivalence ratio (Cassidy 1977)

The bottled hydrogen flow rate was set at a constant value of 0.64 Kg/hour for all equivalence ratios. The mass fraction of the hydrogen did vary slightly with equivalence ratio. A value of 0.068 at the leanest equivalence ratio and 0.063 at the richest. Figure 30 shows that adding hydrogen significantly increases the flame speed at all equivalence ratios but the increase is most pronounced at low equivalence ratios. At an equivalence ratio of 0.68, which is very close to the lean limit for petrol, the addition of hydrogen increases apparent flame speed by 61%.

Cassidy also observed that the higher flame speed resulted in higher combustion temperatures due to the quicker release of the chemical energy in the fuel. This resulted in more energy loss to the cooling system due to the higher temperature gradient, however the higher temperatures also resulted in a more complete burn and an increase in thermal efficiency. At the equivalence ratio of 0.69 where the flame speed is also 61% faster, the energy lost to the exhaust system with the petrol-hydrogen mix, was 37% less than with petrol only (Cassidy 1977, p.14). Cassidy also noted that the total energy consumption at equivalence ratios below 0.7 was significantly lower for both hydrogen-gasoline mixtures at the same flow rate. The conclusion was that only moderate additions of hydrogen are sufficient to allow smooth and efficient lean operation.

Figure 31 shows the improvement in indicated thermal efficiency achieved by the addition of hydrogen to petrol. The hydrogen flow rate of the bottled hydrogen was 0.64 kg/hour and the methanol reformer system was 0.231 kg/hour yet both showed substantial improvement in indicated thermal efficiency especially at low equivalence ratios. At equivalence ratios greater than 0.85 all

the fuels flame speeds increased which caused more energy to be lost to the cooling system. This resulted in a general decrease in thermal efficiency with increased equivalence ratios.

Cassidy also reported that extending the operating range into leaner mixtures by the addition of hydrogen also reduced the formation of NO_x considerably.

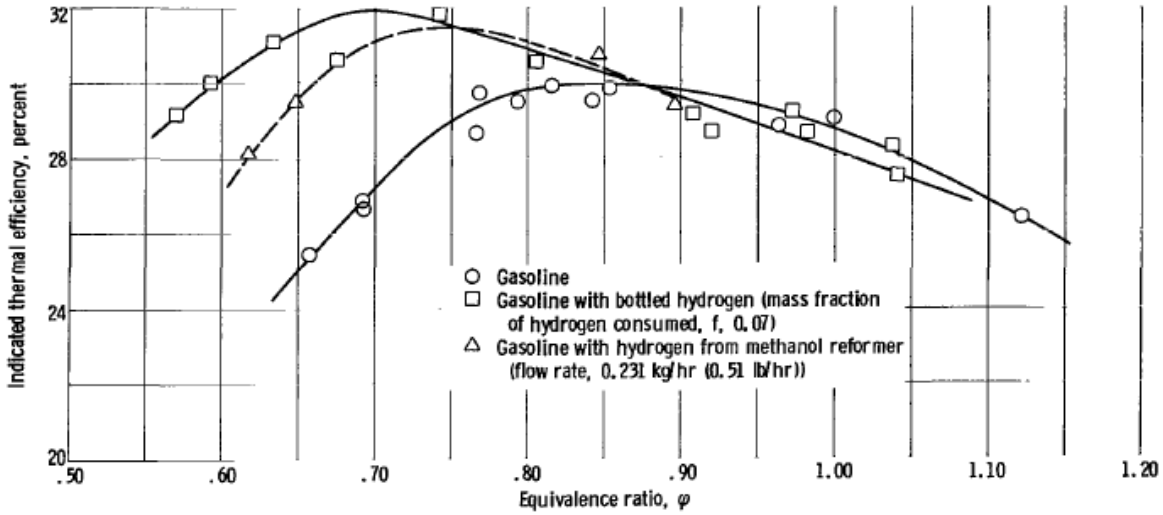

Figure 31 Indicated thermal efficiency as a function of equivalence ratio (Cassidy 1977)

Figure 32 shows a reduction of the NO_x emissions by a factor of 2 when the comparison is made on the basis of minimum energy consumption equivalence ratios of 0.77. If the equivalence ratio is further reduced to 0.6 the NO_x emissions are reduced by a factor of 19, however there is also a 3 to 6 percent increase in energy consumption. Smooth engine operation also deteriorates rapidly as the equivalence ratio drops below the minimum energy consumption value of 0.77.

Additionally Cassidy reported hydrocarbon emissions levels for hydrogen-petrol mix to be slightly higher than petrol only mixtures. This was when compared at the minimum energy consumption equivalence ratio of 0.77. Carbon monoxide levels were very similar for petrol only and reformed hydrogen mixtures and remained low and steady. Petrol with bottled hydrogen produced the lowest carbon monoxide emissions.

On diesel engines similar research was conducted by Midhat et al (2014). The results were similar to those of a petrol engine. Hydrogen (H_2) being a zero carbon fuel and therefore produces no particulate matter, hydrocarbons, carbon monoxide and carbon dioxide(CO_2). Hydrogen has a significantly lower cetane rating than diesel and requires a very low amount of energy to ignite. Hydrogen has a high flame speed compared to hydrocarbon fuels even under very lean conditions. The high flame speed is a result of the fast and thermally neutral branching chain reactions of H_2 compared to the slower endothermic and thermally significant chain reactions associated with hydrocarbon fuel combustion (Midhat et al, 2014, p.2). The high flame speed of hydrogen when co-combusted with diesel fuels tend to increase the overall flame speed of combustion. Faster flame speed results in quicker and more complete release of the thermal energy in the fuels, this allows less time for the heat to flow into the surroundings and as a result thermal efficiency is improved (Midhat et al, 2014, p.2).

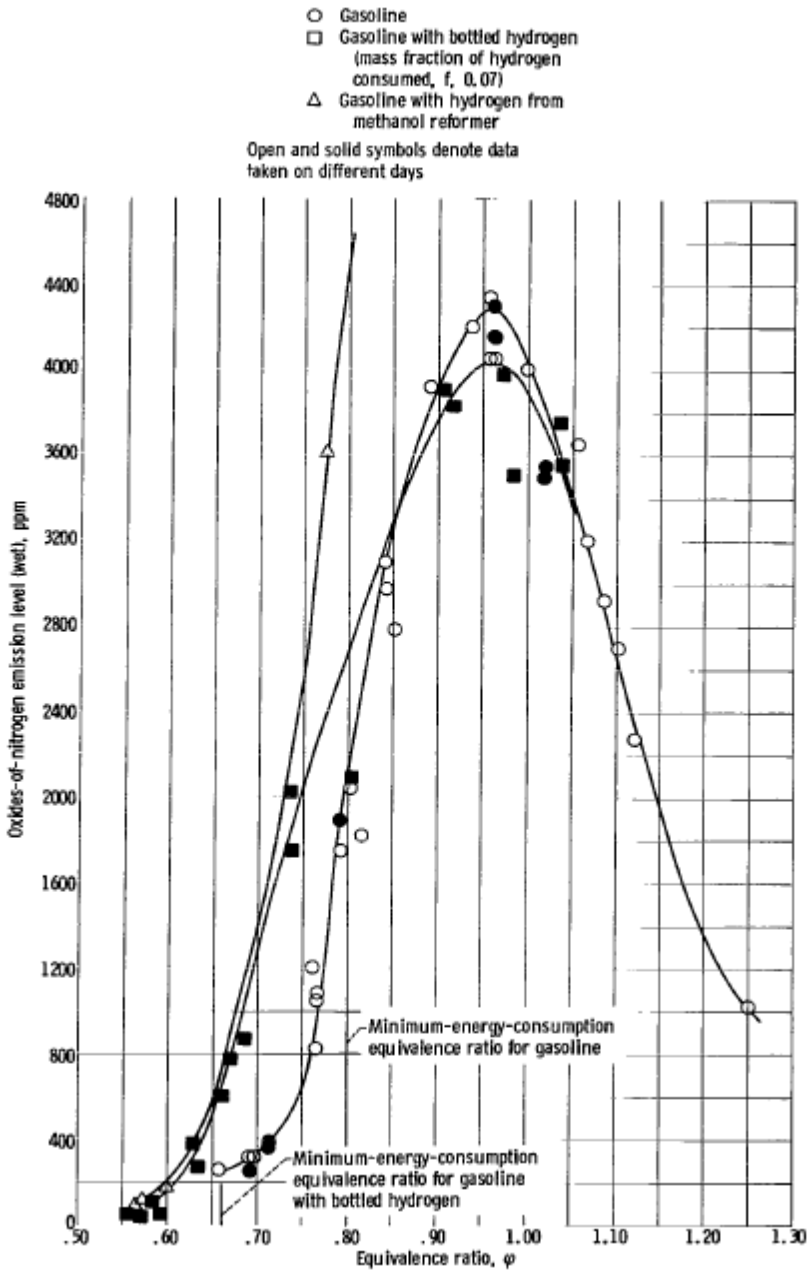

Figure 32 NO_x emission level as a function of equivalence ratio (Cassidy 1977)

Similar research was conducted by Bari and Mohammad Esmaeil (2008) on the effects of H_2/O_2 addition on the thermal efficiency of a diesel engine. The H_2/O_2 generated was by electrolysis from a generator driven by the diesel engine. In this investigation the performance and emission characteristics of a diesel engine were studied using H_2/O_2 mixture enrichment at constant speed of 1500 rpm. The flow rate of the H_2/O_2 mixture was varied to obtain optimal performance at power outputs of 19 Kw, 22 Kw and 28 Kw. The power required to generate the H_2/O_2 was included in the input energy of the engine. The variations in brake thermal efficiency at different % H_2/O_2 mixture are shown in figure 33.

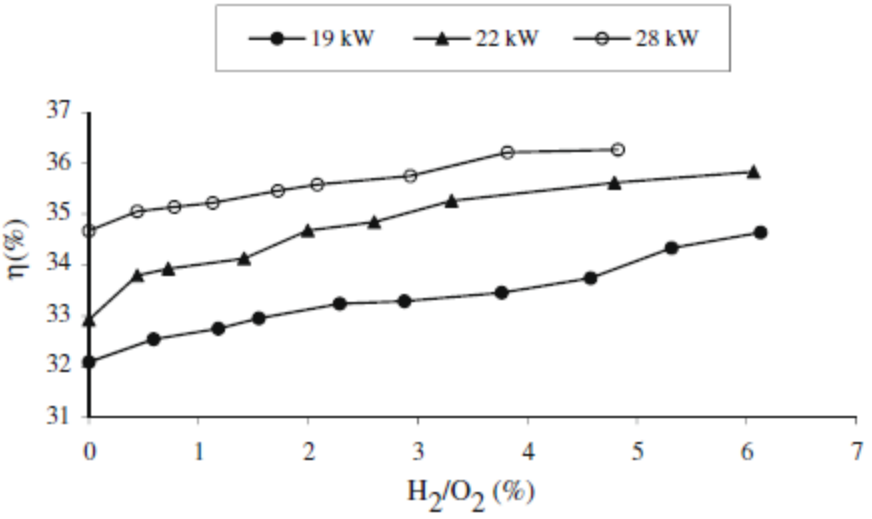

Figure 33 Variation in brake thermal efficiency with H_2/O_2 addition (Bari and Mohammad Esmaeil 2008)

An increase in brake thermal efficiency is noticed as H_2/O_2 level increases for all power levels. The flame speed of hydrogen is 9 times faster than the flame speed of diesel. Combustion of diesel in the presence of hydrogen therefore results in overall faster and more complete combustion (Bari and Mohammad Esmaeil 2008). The result is higher peak pressure closer to TDC which produces a higher effective pressure to do work. These factors were attributed to causing the increase in thermal efficiency. It was also noted that the increase in thermal efficiency diminishes after 5% total diesel equivalent of hydrogen is added.

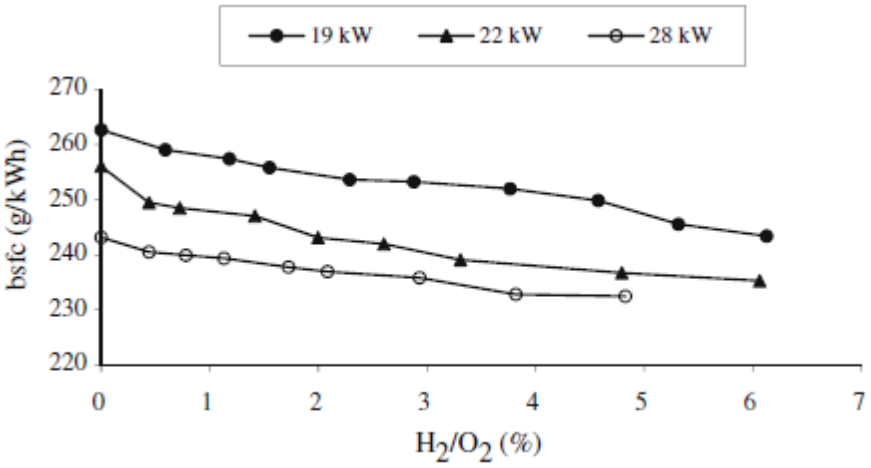

Figure 34 Variation in brake specific fuel consumption with H_2/O_2 addition (Bari and Mohammad Esmaeil 2008)

Figure 34 shows the variation in brake specific fuel consumption with the percentage of H_2/O_2 mixture addition. The fuel consumption is the sum of the diesel, diesel equivalent hydrogen flow rate and diesel equivalent energy needed to produce the H_2/O_2 mixture. Addition of H_2/O_2 mixture into the diesel engine gave fuel consumption improvements of 15.07%, 15.16% and 14.96% at 19Kw, 22Kw and 28Kw respectively. Rate of fuel saving starts to decrease with the addition of more than 4% H_2/O_2 mixture. No significant improvements in fuel consumption were observed beyond 5% addition of H_2/O_2 mixture. Bari and Mohammad Esmaeil concluded that this indicated that beyond 5% mixture addition the H_2/O_2 mixture acted as a fuel rather than as an additive.

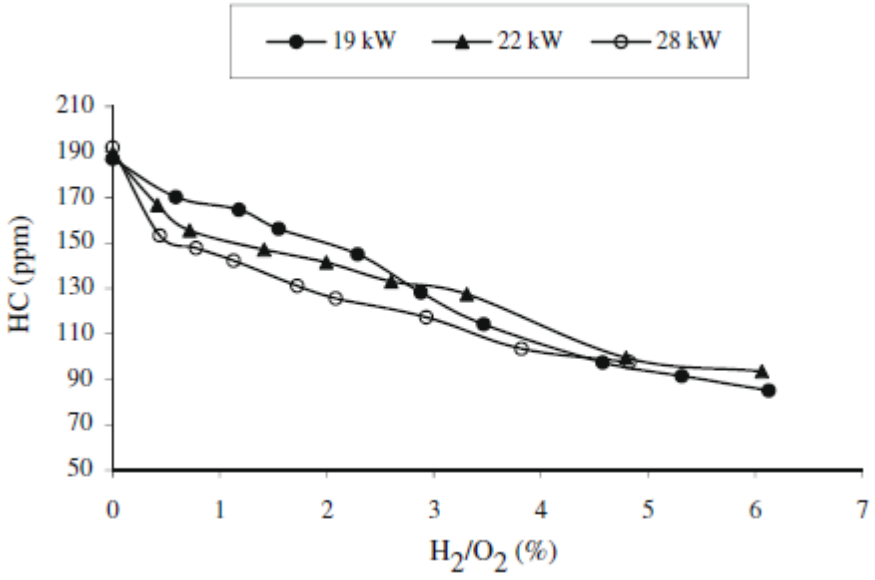

Figure 35 Variation in HC emissions with H_2/O_2 percentage (Bari and Mohammad Esmaeil 2008)

By introducing H_2/O_2 mixture the production of HC emissions is reduced at all power outputs. Maximum reduction of 55% was achieved at the lowest power output of 19Kw. The reduction in HC emissions is due to the absence of carbon in the hydrogen fuel and more complete combustion. Variation in NO_x emission with percentage of H_2/O_2 mixture is shown in figure 36. NO_x emission increased for all load conditions. This is attributed to the higher combustion temperatures as well as the additional O_2 added with the mixture. An average increase in NO_x emission of 28% was noted over all load conditions. Figure 37 shows the variation in carbon monoxide (CO) emissions with percentage of H_2/O_2 mixture. CO emissions are substantially reduced for all load ratings. The maximum reduction of 98% occurred at the lowers load rating.

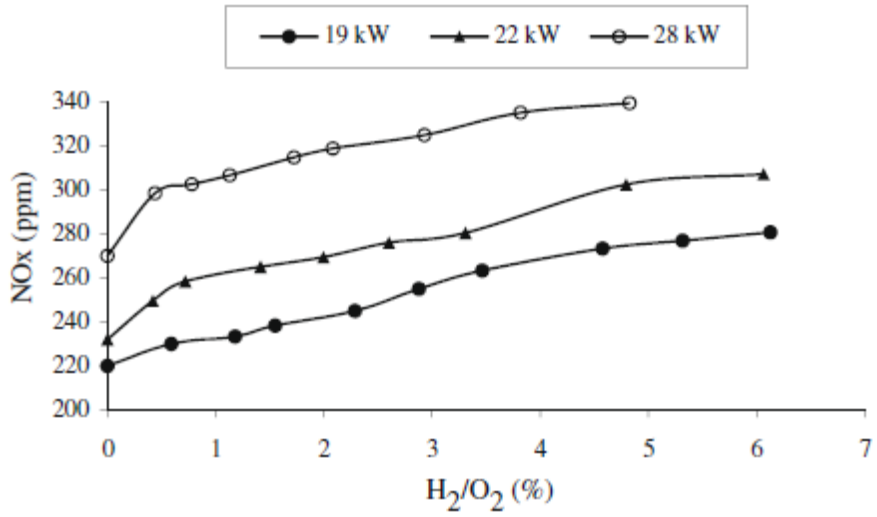

Figure 36 Variation in NO_x emissions with H_2/O_2 percentage (Bari and Mohammad Esmaeil 2008)

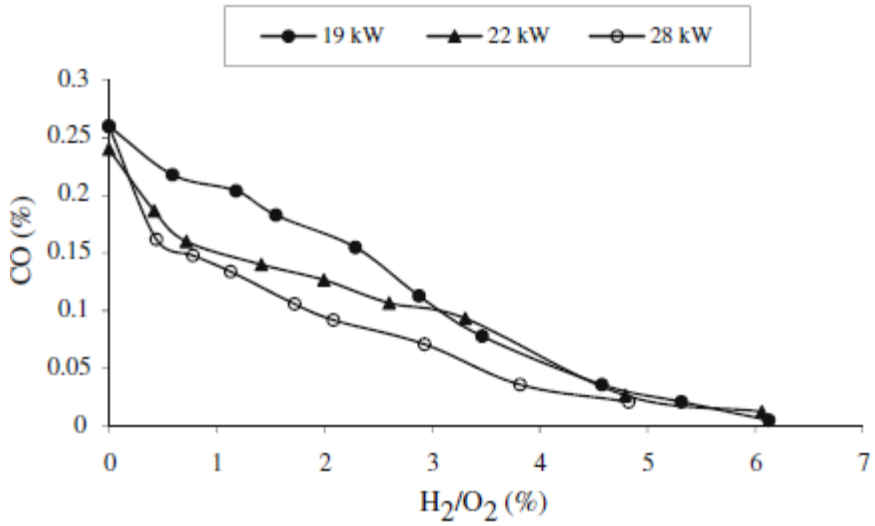

Figure 37 Variation in CO emissions with H_2/O_2 percentage (Bari and Mohammad Esmaeil 2008)

Much accumulated information suggests that co-combustion of hydrogen with hydrocarbon fuel results in a very significant improvement in engine thermal efficiency for both petrol and diesel engines. Under higher load conditions the thermal efficiency drops, and the NO_x emissions in particular, rise. This is largely attributed to the lower flash point of hydrogen causing unstable combustion above a certain load. Unstable combustion and excessive combustion temperatures result in NO_x emissions rising sharply.

It is obvious from the above analysis that introduction of a hydrogen fuel mixture during low load and ultra-lean cruising conditions could result in a significant improvement in fuel economy to both Petrol and Diesel engines. It is also easy to understand why there has been so much debate over whether or not the commercially available systems give any benefit at all. There are many conflicting reports from consumers and suppliers. Some suppliers claim up to 50% improvement in fuel economy and this is verified by some consumers. Some consumers say the system does not work at all and there are dyno test results to prove it.

The idea of hydrogen petrol co-combustion as presented is based on good scientific research but the results are quite clear that for a petrol engine there are only benefits from hydrogen addition under ultra-lean driving conditions. The hydrogen added needs to be operating as an additive and not as a fuel. Modern day vehicle engine management systems keep the equivalence ratio to as close to 1 as practically possible for efficient catalytic convertor operation. Figure 31 shows that at equivalence ratios of close to 1 there is no benefit in hydrogen addition on a petrol engine, but rather a slight drop in thermal efficiency. For an aftermarket hydrogen generator kit to have any benefit the engine management system would need to be remapped to allow ultra-lean conditions when cruising and control the addition of hydrogen during these conditions only. Diesel engines appear to have benefits at all moderate load conditions.

5.3.2 Electrolysis

Hydrogen does not occur naturally in its molecular structure in nature. Hydrogen needs to be produced by a process and energy input. To date hydrogen is mostly produced by a process called steam reformation. Steam reformation is a process whereby water vapor at high temperatures $(700{\sim}1100℃)$ is reacted with fossil fuels in the presence of a metal based catalyst. Steam reforming of fossil fuels produces low purity hydrogen with a high content of carbon based species such as carbon monoxide. Additionally steam reforming does not reduce dependency on already scarce fossil fuel reserves (Carmo et al 2013).

High quality hydrogen of 100% purity can be produced by electrochemical conversion of water into hydrogen and oxygen by electrolysis. The reaction with energy values is given in equation 5.1.

5.1

$$\boldsymbol{H_2O_{Liquid} + 237.2kjmol^{-1}{}_{electricity} + 48.6kjmol^{-1}{}_{heat} \rightarrow H_2 + 0.5O_2}$$

There are few different electrolysis techniques used for the production of hydrogen. The main ones are alkaline water electrolysis, Solid oxide electrolysis (SOEC) and Polymer electrolyte membrane (PEM). Alkaline water electrolysis is the most common electrolysis technique on a commercial level worldwide (Carmo et al 2013). It is characterized by two electrodes immersed in a liquid alkaline electrolyte consisting of a caustic potash solution at $20{\sim}30\%\ KOH$. The electrodes are separated by a diaphragm which keep the resulting oxygen and hydrogen separate from each other which maintains efficiency and safety. Major issues associated with alkaline electrolyzes are:

- Low partial load range

- Limited current density
- Low operating pressure
- Inefficient diaphragm sealing

Polymer electrolyte membrane (PEM) electrolysis was first noted by General Electric in the 1960s and has been refined since then. The system consists of a solid sulfonated polystyrene membrane which is used as an electrolyte. The polymer electrolyte membrane provides high proton conductivity, low gas crossover, compact system design and high pressure operation (Carmo et al 2013). PEM can achieve higher current densities and lower crossover rates yielding purer hydrogen more safely. The response to load changes is quicker than alkaline electrolysis. Most high range hydrogen generators for automotive application are of the PEM type. A comparison between the advantages and disadvantages of the electrolysis techniques is shown in Table 22.

Table 22 Advantages and disadvantages of electrolysis techniques (Carmo et al 2013)

Alkaline electrolysis	PEM electrolysis	SOEC electrolysis
Advantages		
Well established technology	High current densities	Efficiency up 100%; thermoneutral
Non noble catalysts	High voltage efficiency	Efficiency >100% w/hot steam
Long-term stability	Good partial load range	Non noble catalysts
Relative low cost	Rapid system response	High pressure operation
Stacks in the MW range	Compact system design	
Cost effective	High gas purity	
	Dynamic operation	
Disadvantages		
Low current densities	High cost of components	Laboratory stage
Crossover of gases (degree of purity)	Acidic corrosive environment	Bulky system design
Low partial load range	Possibly low durability	Durability (brittle ceramics)
Low dynamics	Commercialization	No dependable cost information
Low operational pressures	Stacks below MW range	
Corrosive liquid electrolyte		

Table 23 Comparison of performance between alkaline electrolysis and PEM (Carmo et al 2013)

Specifications	Alkaline electrolysis	PEM electrolysis
Cell temperature (°C)	60–80	50–80
Cell pressure (bar)	<30	<30
Current density (mA cm^{-2})	0.2–0.4	0.6–2.0
Cell voltage (V)	1.8–2.4	1.8–2.2
Power density (mW cm^{-2})	<1	<4.4
Voltage efficiency HHV (%)	62–82	67–82
Specif. energy consumption: Stack (kW h Nm^{-3})	4.2–5.9	4.2–5.6
Specif. energy consumption: System (kW h Nm^{-3})	4.5–7.0	4.5–7.5
Lower partial load range (%)	20–40	0–10
Cell area (m^2)	>4	<0.03
H_2 production rate: Stack-system (Nm^3 h^{-1})	<760	<10
Lifetime stack (h)	<90,000	<20,000
Lifetime system (y)	20–30	10–20
Degradation rate (μV h^{-1})	<3	<14

5.3.3 Output analysis

Given in Table 20 that a PEM hydrogen generator requires 4.5 $KW.h/Nm^3$ and that the exhaust gas thermal generator presented can produce 1.552KW at optimum performance.

then:

PEM hydrogen generator efficiency = 4.5 $KW.h/Nm^3$ (Table 23)

Where Nm^3 stands for normal m^3 which is at 101.325 KPa and 273K.

Exhaust thermal generator power = 1.552 KW

$$\frac{4.5}{1.552} = 2.706\ Hours/Nm^3$$

$$0.37Nm^3/hour$$

Using gas law equation

5.2

$$\boldsymbol{PV = mRT}$$

where

P = absolute pressure in Pa

V = Volume in m^3

m = mass of hydrogen kg

R = specific gas constant $J/kg\ K$

T = temperature

$$m(H_2) = \frac{PV}{RT}$$

$$m(H_2) = \frac{101325 \times 0.37}{4120 \times 273}$$

$$\boldsymbol{m(H_2) = 0.033kg/hour}$$

The total mass of $\mathrm{H_2/O_2}$ mixture given that the molar mass of oxygen is 16 time greater than hydrogen would be.

$$m(\mathrm{H_2/O_2}) = 0.033 + (0.033 \times 8)$$

$$\boldsymbol{m(\mathbf{H_2/O_2}) = 0.297kg/hour}$$

The research conducted by Bari and Mohammad Esmaeil found that the optimum $\mathrm{H_2/O_2}$ mixture for the 4 L diesel engine used in there tests, was approximately 25 l/min or 0.025 m^3/min. Assuming that this flow was at 300K then:

$$m(H_2/O_2) = \frac{101325 \times 0.025}{4120 \times 300}$$

$$m(H_2/O_2) = 0.002kg/min$$

$$\boldsymbol{m(H_2/O_2) = 0.123kg/hour}$$

The results of the analysis show that the thermal electric generator operating on the expected output of 1552 watts should be able to produce $0.297kg/hour$ of $\mathrm{H_2/O_2}$ mixture. The estimated requirement based on the tests done by Bari and Mohammad Esmaeil was $0.123kg/hour$. It is therefore concluded that that a thermal electric generator of this power output should be capable of supplying sufficient hydrogen/oxygen mixture for Continuous operation.

The maximum increase in brake thermal efficiency found by Bari and Mohammad Esmaeil was at 22Kw and found to increase from 32.9% to 35.8% (Figure 21). The flow rate of $\mathrm{H_2/O_2}$ mixture to obtain

this increase in efficiency was 29.8 l/min. In this test the power to produce the 29.8 l/min came from the engine power output.

Engine power output to produce 29.8 l/min $= 1.552 \times (0.123 \times 29.8/25)/0.297$

$= \mathbf{0.766}\boldsymbol{Kw}$

Increase in total thermal efficiency if power to create H_2/O_2 mixture was obtained from the thermal electric generator.

Total Thermal efficiency $= ((22 + 0.766) \times 0.358)/22$

Total Thermal efficiency $=$ **37%**

Percentage increase in total thermal efficiency with thermal electric powered hydrogen generator.

Increase in total thermal efficiency $= (37 - 32.9)/32.9$

Increase in total thermal efficiency $=$ **12.5%**

The results of this basic analysis show that a thermal electric generator as proposed in this project should produce enough power to charge a vehicle battery as well as power a hydrogen generating cell and potentially increase the engines thermal efficiency by 12.5%. Effectively recycling of exhaust gas thermal waste could improve the overall thermal efficiency of the engine as shown in Figure 38 and Figure 39.

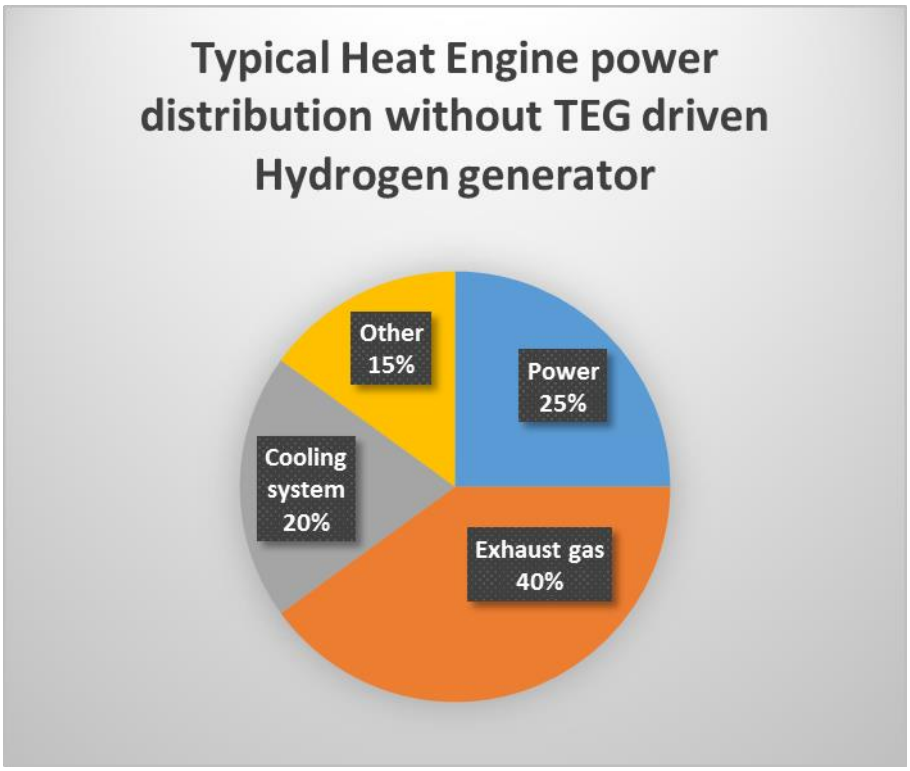

Figure 38 Heat power distribution without TEG driven hydrogen generator.

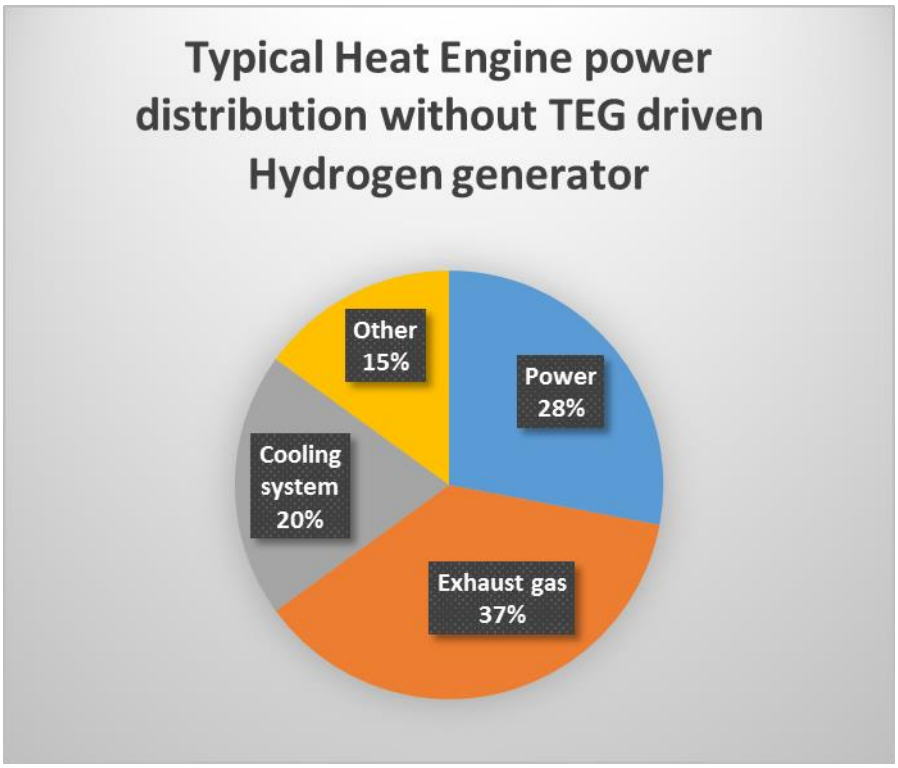

Figure 39 Heat power distribution with TEG driven hydrogen generator.

Chapter 6

Conclusion

6.1 Introduction

Heat waste is an unavoidable consequence of extracting mechanical or electrical power from a heat source. In an internal combustion engine the major components of the heat waste is in the form of hot exhaust gases and transient heat energy dissipated by the cooling system. Recycling of this low quality thermal energy is becoming increasingly viable with the ever increasing efficiency levels of thermoelectric generators. Engineers have traditionally tried to reduce wasted thermal energy by attempting to improve engine thermal efficiency. After 100 years of engine development thermal efficiency level are in the region of 25 to 35%. Improvements in efficiency are becoming harder and harder to achieve. Use of wasted thermal energy can at least result in improvements in overall efficiency.

The use of a thermal generator to replace the vehicle charging system is a feasible concept. If we take an alternator charging system at maximum power able to produce $100A$ at $12.6V$. The resulting power is $1260W$, which is close to the estimated power output of the thermal generator of $1552W$. The fact that a thermal generator has no moving part and is driven by what would be wasted energy, makes the technology very attractive for future application. Especially considering that TEG thermal efficiency is still expected to improve further (Lusheng SU et al, 2011)

The use of a thermal generator to power a hydrogen producing cell to improve low load engine efficiency and fuel consumption is a sound concept in principle. According to the results of tests already conducted it would appear that the power required by the thermal generator presented in this particular design would be sufficient to maintain vehicle battery charge as well as power a hydrogen producing cell. The resulting addition of hydrogen to the vehicle fuel system as an additive could increase the engines brake thermal efficiency by 12.5%

Additional research needs to be conducted to ascertain what the optimal hydrogen addition ratio would be for varies engine types and loading conditions. Additionally the thermal generator design presented was only extracting waste heat from the exhaust system. There is almost the same amount of thermal waste energy in the cooling system that has not been considered in this report. Use of the cooling system waste heat could almost double the generator power output. The design of the exhaust gas thermal electric generator presented has also not been optimized, and it is expected that the layout efficiency and configuration may be improved. The TEG modules selected for the design (BiTe-PbTe hybrid) had an upper temperature limit of $350℃$ and a thermal efficiency of 7%. The exhaust gas temperatures could be significantly higher than $350℃$, especially under load. For practical application this upper temperature limit would need to be improved to allow reliable operation.

As efficiency levels of TEG improve, and all sources of waste thermal energy are utilized (cooling system). Extra power should become available and the use of TEG to improve lean burn

combustion efficiency by hydrogen generation as well as to replace a conventional alternator charging system, may become a viable proposition.

Appendix A – Project Specifications

University of Southern Queensland

Faculty of Engineering and Surveying

ENG 4111/4112 Research Project

For:	Andrew Bellars
Topic:	Vehicle Energy Usage
Supervisor:	Dr Ray Malpress
Enrolment:	ENG 4111 S1 2015
	ENG 4112 S2 2015
Project Aim:	Assess the current level of efficiency of energy usage in motor vehicle and internal combustion engines. Compare with theoretically achievable levels. Energy balance. Evaluate opportunities for recycling of waste heat. Suggest potential solutions and verify viability.
Programme:	Version 1 (12/03/15)

1) An analysis of current vehicle energy system usage and efficiencies.
2) Thermal efficiency of IC engine / Air Standard efficiency / limits / energy lost.
3) Discussion on energy quality / Carnot efficiency / Otto cycle air standard efficiency
4) Waste heat energy in Automotive IC engine application / Exhaust system / Cooling systems. Driveline losses / Torque convertor / braking systems. Energy balance of varies systems. Discussion on how much energy is actually wasted and what is the potential for recycling.
5) Current thermal generator technology. Seebeck effect in particular
6) Proposal for exhaust system waste heat extraction and usage potential using current thermal generator technology. Produce a proposed model and design of an exhaust system designed for electricity generation using current thermal generator technology. Produce heat flow analysis of exhaust system and estimate potential electric power generated
7) Discuss potential uses for recycled heat/electrical energy i.e. Battery charging system / fuel booster via electrolysis.

Agreed:

Student (Andrew Bellars) signed _____ date / /

Supervisor (Dr Ray Malpress) signed _____ date / /

Examiner (Dr Chris Snook) signed _____ date / /

References

JM Clutches and converters 2013
http://jmclutch.com/site/book/export/html/7

http://user.physics.unc.edu/~rowan/p24site/p24units/unit18/FG18_16.JPG

http://hyperphysics.phy-astr.gsu.edu/hbase/thermo/imgheat/carnot.gif

http://web.mit.edu/16.unified/www/FALL/thermodynamics/notes/node26.html

http://espressomilkcooler.com/about/

The Energy story 2012 , California Energy Commission,
http://energyquest.ca.gov/story/chapter18.html

Da Rosa, Aldo V, 18 Dec 2012, Fundamentals of Renewable Energy Processes.

Yunus A. Cengel, Michael A. Boles, 2002, Thermodynamics an engineering approach

Lee, Ho Sung, September 2010, Thermal design

DM. Rowe, G. Min, 1998, Evaluation of thermoelectric modules for power generation

McDonald J & Jones L 2000 'Demonstration of Tier 2 Emission levels for heavy light duty trucks', *SAE technical paper series*, 2000-01-1957

Suzuki T & Sakurai Y 2006 'Effect of Hydrogen rich gas and gasoline mixed combustion on spark ignition engine', *SAE technical paper series*, 2006-01-3379

Midhat T, Hellier P, Balachandran R, Ladommatos N 2014 'Effect of hydrogen-diesel co-combustion on exhaust emissions with verification using an in cylinder sampling technique' , *International journal of hydrogen energy*, 30 April 2014

Bari S, Mohammad Esmaeil M, 2008,'The effect of H_2 and O_2 addition in increasing of the thermal efficiency of a Diesel engine', *School of Advanced Manufacturing and Mechanical Engineering, University of South Australia*

Middleman V & Wagner U 2010 ‘The Torque converter as a system’, Http://www.schaeffler.com

Dr Faust IH, 2014,’Power train systems of the future’, *10th Schaeffer symposium*, 3 April 2014

Mazloomi K, Sulaiman NB, Moayedi H, 2012,’Electrical efficiency in electrolytic hydrogen production’, *International journal of electrochemical science*, 1 April 2012

Cassidy JF, 1977, ‘Emissions and total energy consumption of a multicylinder piston engine running on gasoline and hydrogen gasoline mixture’, *National Aeronautics and Space Administration,* May 1977

Carmo M, Fritz DL, Mergel J, Stolten D, ‘A comprehensive review of PEM water electrolysis’, *International Journal of Hydrogen Energy, 19 January 2013*

Shengqiang B, Hongliang L, Ting W, Xianglin Y, Xun S, Lidong C, ‘*Numerical and experimental analysis for exhaust heat exchangers in automobile thermoelectric generators’, Case Studies in Thermal Engineering, 9 July 2014*

Rashid M, 2011*, ‘Power electronics handbook Third Edition’*

Braess HH, Seiffer U, 2005, ‘*Handbook of Automotive Engineering’, USA: SAE International*

Lusheng SU, Yong X, 2011, ’*Advances in Thermoelectric Energy Conversion Nanocomposites’, Department of Mechanical Engineering, University of Toledo*